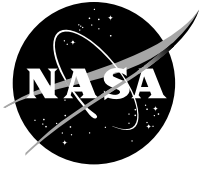# Rolling-Element Fatigue Testing and Data Analysis—A Tutorial

Brian L. Vlcek
Georgia Southern University, Statesboro, Georgia

Erwin V. Zaretsky
Glenn Research Center, Cleveland, Ohio

NASA STI Program . . . in Profile

Since its founding, NASA has been dedicated to the advancement of aeronautics and space science. The NASA Scientific and Technical Information (STI) program plays a key part in helping NASA maintain this important role.

The NASA STI Program operates under the auspices of the Agency Chief Information Officer. It collects, organizes, provides for archiving, and disseminates NASA's STI. The NASA STI program provides access to the NASA Aeronautics and Space Database and its public interface, the NASA Technical Reports Server, thus providing one of the largest collections of aeronautical and space science STI in the world. Results are published in both non-NASA channels and by NASA in the NASA STI Report Series, which includes the following report types:

- TECHNICAL PUBLICATION. Reports of completed research or a major significant phase of research that present the results of NASA programs and include extensive data or theoretical analysis. Includes compilations of significant scientific and technical data and information deemed to be of continuing reference value. NASA counterpart of peer-reviewed formal professional papers but has less stringent limitations on manuscript length and extent of graphic presentations.

- TECHNICAL MEMORANDUM. Scientific and technical findings that are preliminary or of specialized interest, e.g., quick release reports, working papers, and bibliographies that contain minimal annotation. Does not contain extensive analysis.

- CONTRACTOR REPORT. Scientific and technical findings by NASA-sponsored contractors and grantees.

- CONFERENCE PUBLICATION. Collected papers from scientific and technical conferences, symposia, seminars, or other meetings sponsored or cosponsored by NASA.

- SPECIAL PUBLICATION. Scientific, technical, or historical information from NASA programs, projects, and missions, often concerned with subjects having substantial public interest.

- TECHNICAL TRANSLATION. English-language translations of foreign scientific and technical material pertinent to NASA's mission.

Specialized services also include creating custom thesauri, building customized databases, organizing and publishing research results.

For more information about the NASA STI program, see the following:

- Access the NASA STI program home page at *http://www.sti.nasa.gov*

- E-mail your question via the Internet to *help@ sti.nasa.gov*

- Fax your question to the NASA STI Help Desk at 443–757–5803

- Telephone the NASA STI Help Desk at 443–757–5802

- Write to:
  NASA Center for AeroSpace Information (CASI)
  7115 Standard Drive
  Hanover, MD 21076–1320
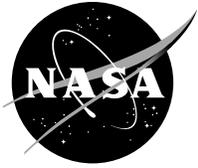
Rolling-Element Fatigue Testing and Data Analysis—A Tutorial

Brian L. Vlcek
Georgia Southern University, Statesboro, Georgia

Erwin V. Zaretsky
Glenn Research Center, Cleveland, Ohio

National Aeronautics and
Space Administration

Glenn Research Center
Cleveland, Ohio 44135

March 2011

Rolling-Element Fatigue Testing and Data Analysis—A Tutorial

Brian L. Vlcek
Georgia Southern University
Statesboro, Georgia 30458

Erwin V. Zaretsky[*]
National Aeronautics and Space Administration
Glenn Research Center
Cleveland, Ohio 44135

Abstract

In order to rank bearing materials, lubricants and other design variables using rolling-element bench type fatigue testing of bearing components and full-scale rolling-element bearing tests, the investigator needs to be cognizant of the variables that affect rolling-element fatigue life and be able to maintain and control them within an acceptable experimental tolerance. Once these variables are controlled, the number of tests and the test conditions must be specified to assure reasonable statistical certainty of the final results. There is a reasonable correlation between the results from elemental test rigs with those results obtained with full-scale bearings. Using the statistical methods of W. Weibull and L. Johnson, the minimum number of tests required can be determined. This paper brings together and discusses the technical aspects of rolling-element fatigue testing and data analysis as well as making recommendations to assure quality and reliable testing of rolling-element specimens and full-scale rolling-element bearings.

Nomenclature

A area due to plastic deformation and wear, m^2, (in.^{2})

C confidence number, fractional percent or percent

e Weibull slope or Weibull modulus

F probability of failure $(1 - S)$, fractional percent

H depth of stressed surface due to plastic deformation and wear, maximum distance from chord to contact surface, m, (in.)

h' distance from chord to original surface, m, (in.)

j sequential failure number where $j = 1,2,3,...r$

L life, revolutions, stress cycles or hours.

L_{10} 10-percent life or life at which 90-percent of population survives, revolutions, stress cycles or hours

L_{50} median life or life at which fifty percent of a population fails, revolutions, stress cycles or hours

L_β characteristic life or life at which 63.2 percent of population fails, revolutions, stress cycles or hours

L_μ location parameter or life below which no failures will occur, revolutions, stress cycles or hours

l 1/2 chord length, m, (in.)

m total number of bearings or specimens in a subgroup, number of bearing testers

n number of data sets, test series, or samples

P_t thrust load, N, (lb)

P_r radial load, N, (lb)

R original radius or curvature, m, (in.)

---

[*]Distinguished Research Associate.

R_p profile radius, m, (in.)

r number of failures or number of subgroups

S probability of survival $(1 - F)$, fractional percent

S_{90} 90-percent probability of survival, fractional percent

ω rotational speed, rpm

Subscripts:

ir inner race

or outer race

re rolling element

x probability of survival

Introduction

While there can be multiple failure modes of rolling-element bearings, the ultimate failure mode limiting bearing life is contact (rolling-element) surface fatigue of one or more of the running tracks of the bearing components. Rolling-element fatigue is extremely variable but is statistically predictable depending on the material (steel) type, the processing, the manufacturing, and operating conditions (Ref. 1). Sadeghi, et al. (Ref. 2) provide an excellent review of this failure mode. Alley and Neu (Ref. 3) provide a recent attempt at modeling rolling-element fatigue. With improved manufacturing and material processing, the potential improvement in bearing life can be as much as 80 times that attainable in the late 1950s or as much as 400 times that attainable in 1940 (Ref. 4).

In 1896, R. Stribeck (Ref. 5) in Germany began fatigue testing full-scale rolling-element bearings. Rolling-element fatigue life analysis is based on the initiation or first evidence of fatigue spalling on a loaded, contacting surface of a bearing. This spalling phenomenon is load cycle dependent. Generally, the spall begins in the region of maximum shearing stresses, located below the contact surface, and propagates into a crack network. Failures other than that caused by classical rolling-element fatigue are considered avoidable if the component is designed, handled, and installed properly and is not overloaded (Ref. 1). However, under low elastohydrodynamic (EHD) lubricant film thickness conditions, rolling-element fatigue can be surface or near-surface initiated with the spall propagating into the region of maximum shearing stresses. C.A Moyer and E.V. Zaretsky discuss in detail "failure modes related to bearing life" in Reference 1.

The database for ball and roller bearing fatigue testing is extensive. A concern that arises from these data and their analysis is the variation between life calculations and the actual endurance characteristics of these components. Experience has shown that endurance tests of groups of identical bearings under identical conditions can produce a variation in life at a 90-percent probability of survival (L_{10} life) from group to group. If a number of apparently identical bearings are tested to fatigue at a specific load, there is a wide dispersion of life among these bearings. For a group of 30 or more bearings, the ratio of the longest to the shortest life may be 20 or more (Ref. 1). This variation can exceed reasonable engineering expectations.

Variables affecting rolling-element fatigue have been experimentally studied and documented by many investigators for over 100 years. In 1963, J.E. Moult (Ref. 6) discussed the then known variables that affect rolling-element fatigue life. He concluded that, "*Qualitative comparisons of bearing performance require test bearing and test conditions to be statistically equivalent at all stages of processing, including the material, except for the variable being compared. Quantitative comparisons have the additional requirement that the results must be related to the performance of a control bearing sample in combination with a control lubricant.*" *A* compilation of those variables that effect rolling-element fatigue life were codified in Reference 7 as ASME life modifying factors to the then existing ISO

and ANSI/ABMA rolling bearing life prediction standards. Later these variables were expanded by the STLE to become more inclusive (Ref. 1). The life modifying factors were updated from those of Reference 7 to reflect the then existing data base (Ref. 1).

In order to rank bearing materials, lubricants and design variables using rolling-element bench type fatigue testing and full-scale rolling-element bearing tests, the investigator needs to be aware of the variables that effect rolling-element fatigue life, and to be able to maintain and control them within an acceptable experimental tolerance. Once these variables are controlled, the number of tests and the test conditions need to be specified to assure reasonable statistical certainty of the final results. Using the statistical methods of W. Weibull (Refs. 8 and 9) and L. Johnson (Ref. 10), the minimum number of tests required can be determined.

There is reasonable correlation between the results from elemental test rigs with those results obtained with full-scale bearings. It is the objective of the work reported herein to bring together and discuss the technical aspects of rolling-element fatigue testing as well as making recommendations to assure quality and reliable testing of rolling-element specimens and full-scale rolling-element bearings.

Rolling-Element Fatigue Testing

Bench-Type Fatigue Testers

The determination of the rolling-element fatigue life of a bearing made from a particular steel or the effect of a specific lubricant on fatigue life is an expensive undertaking. Very high scatter or dispersion in fatigue life makes it necessary to test a large number of specimens. The cost is high both in money and time. This is borne out by the fact that a high-quality aircraft bearing can cost upwards of several thousand dollars each and run for several thousand hours. Bearing companies and various research laboratories have pioneered the use of bench type rolling-element fatigue testers which can simulate to various degrees the conditions found under full-scale bearing operation. Generally, these test rigs perform accelerated rolling-element fatigue testing of element specimens such as a ball or a roller at maximum Hertz (compressive) stress levels beyond 4.14 GPa (600 ksi).

The results obtained with the bench type testers have been used to indicate trends and to rank materials and lubricants. The vast majority of published data have been obtained in bench type fatigue testers. The results from these testers qualitatively, although not necessarily quantitatively, compare with test results from full-scale bearing tests (Ref. 11).

The best compendium of rolling-element fatigue testing and types of bench type rolling-element fatigue testers was that compiled by J.J.C. Hoo (Ref. 12) for the American Society for Testing Materials (ASTM). The more commonly used test rigs discussed in Reference 12 are (a) Two-disk Machine or Ring-to Ring Rolling-Contact Fatigue Tester, (b) Barwell Four-Ball Fatigue Tester, (c) NASA Spin Rig, (d) Pratt-Whitney One-Ball Fatigue Tester (Fig. 1), (e) General Electric R-C (Rolling-Contact) Tester (Fig. 2), (f) NASA Five-Ball Fatigue Tester (Fig. 3), (g) Unisteel Flat Washer Fatigue Tester, (h) Federal-Mogul Ball-Rod Rolling-Contact Fatigue (*RCF*) Tester, (i) NTN Cylinder-to-Ball Rolling-Contact Fatigue Tester, and (j) NTN Cylinder-to-Cylinder Rolling Contact Fatigue Tester. These test rigs employ an automatic failure detection and shutdown system.

Lubrication mode for the test specimen depends on the type of test rig and the operating conditions. The lubrication mode can be by oil mist, oil jet (recirculating oil system), oil drip, or oil bath. Once-through, oil-mist lubrication for these types of tests appears to be the most efficient lubrication mode. After each test the oil should be discarded and not reused. However, a sample of oil from each test should be saved and cataloged for later laboratory analysis, if necessary.
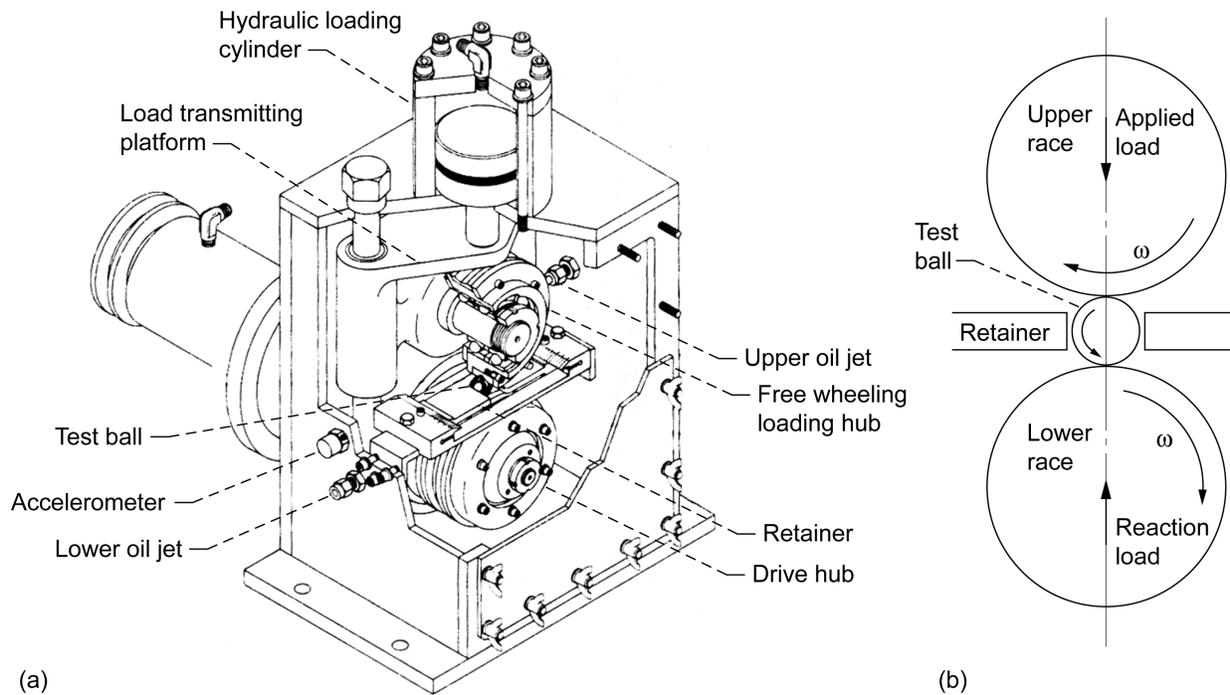
Figure 1.—P&W one-ball fatigue tester (Ref. 12). (a) Test apparatus. (b) Test-specimen assembly.
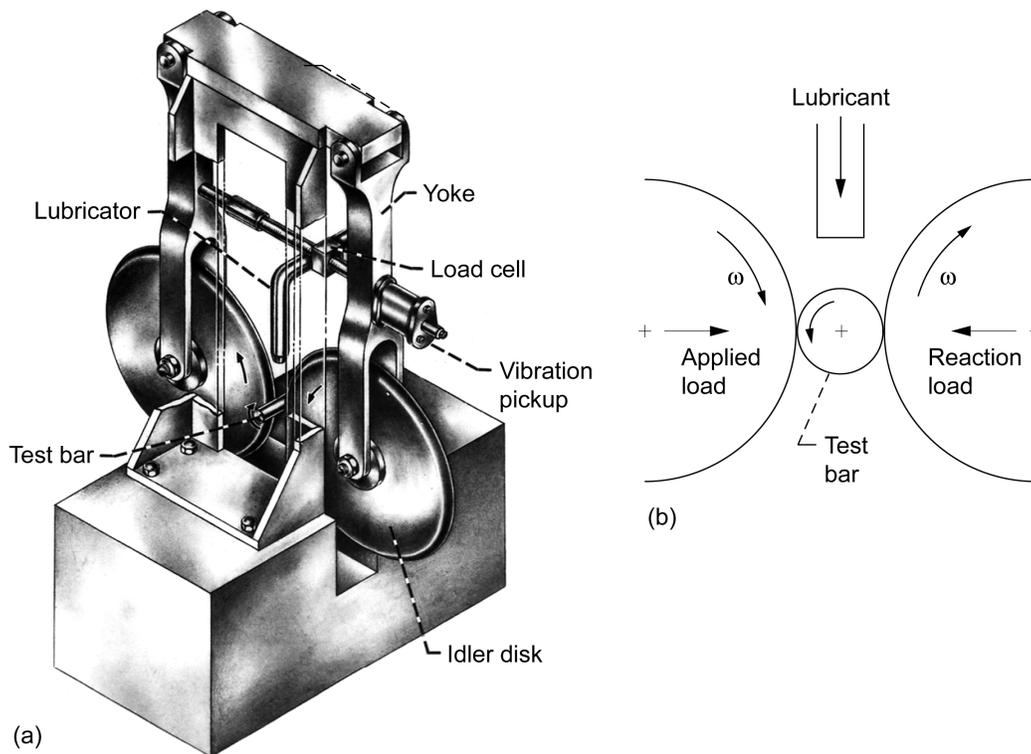

Figure 2.—GE Rolling-Contact (RC) fatigue tester (Ref. 12). (a) Test apparatus. (b) Test-specimen assembly.
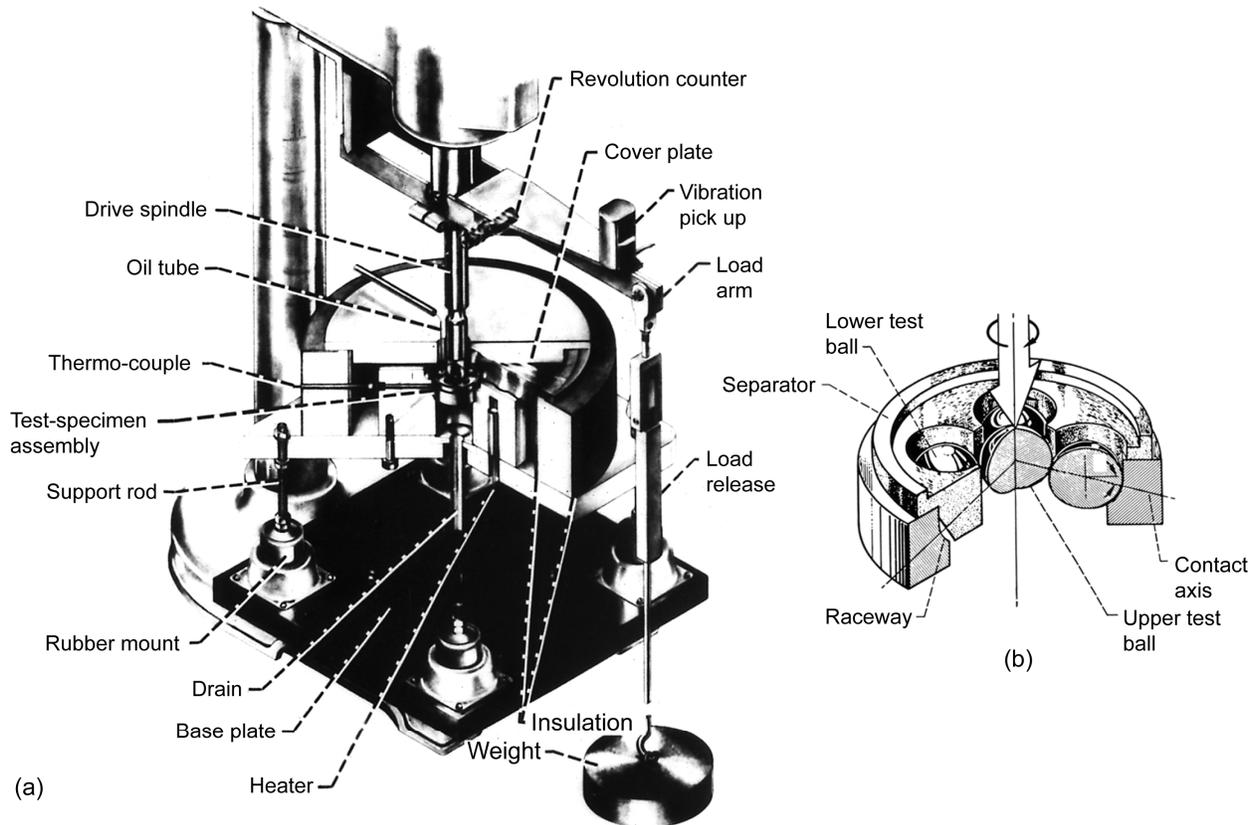
Figure 3.—NASA Five-Ball fatigue tester (Ref. 12). (a) Test apparatus. (b) Test-specimen assembly.

Test Procedures for Bench Type Testers

When testing in a bench-type rig, various precautions must be taken in order to obtain valid comparison of the lubricant, material, and/or operating variables. The procedure as outlined is that followed by the authors and other investigators who have conducted a considerable number of rolling-element fatigue studies. It is mandatory, first of all, to have all the rolling-element specimens fabricated from a single heat of material and heat treated simultaneously to the same hardness. All specimens must have the same surface finish unless, of course, the surface finish is the parameter being studied. The steel microstructure should be reported together with the retained austenite and residual stress before and after testing. It is of prime importance that the difference in hardness between the contacting test specimens remains constant.

Prior to test, all contacting elements should be cleaned thoroughly with a solvent and wiped dry with a clean cloth. Subsequently, the mating elements should be coated with the test lubricant and installed in the tester.

Lubricant flow into the test assembly should be monitored. In addition, the specimens should be loaded prior to start-up. If no load is placed on the specimens prior to starting the test, damage can result due to skidding of the contacting surfaces. Speed and test temperature should be periodically monitored during the testing. Subsequent to testing, all specimens should be examined and their condition recorded. It has been the authors' experience that 30 specimens should be run for a given series of tests anticipating that at least one-third to one-half of the specimens will fail. Care must be taken to make sure that, in any series of tests in which material parameters are compared, all test are conducted with the same lubricant formulation obtained from the same lubricant batch. The same lubricant obtained from different batches can give significantly different results. In testers where mating elements are not replaced subsequent to test, the elements must be examined to make sure that they have not been damaged during prior operation.

Where elevated temperature tests are to be conducted it is a general procedure to heat the specimen housing prior to beginning a test. Before start-up, the lubricant flow is begun to make sure that there is a sufficient amount of lubricant in the test system to prevent wear at startup.

It is generally a good idea, where material comparisons are to be made, that the lubricant has good storage stability. It has been the authors' experience that super-refined mineral oils of the paraffinic or naphthenic type and polyalphaolefin (PAO) are stable over extremely long periods of time and can give consistent results, making material comparisons possible. However, when using ester based lubricants, long term stability of the lubricant must be considered. To avoid water absorption, the lubricant should not be exposed to the atmosphere for any length of time. During storage, the lubricant must be kept under an inert cover gas.

For a given type fatigue tester where there are multiple rigs and/or multiple test heads being used, it is prudent to assure that each test rig and/or test head is providing the same test results. This assures that there are no sources of random variability or systematic differences between the test rigs and/or test heads (Ref. 13). Because wear out of the test apparatus is a random variable, these comparisons need to be made on a continuous basis.

Deformation Effects on Contact Geometry and Stress

In order to obtain rolling-element fatigue data in a bench-type, rolling-element fatigue test rig within a reasonable time, the maximum Hertz test stresses that are used are generally at or above the static load capacity of the hardened bearing steel surface at which plastic deformation will occur. Besides plastic deformation, experience has shown that fracture of the contacting surfaces may occur at maximum Hertz stresses at or beyond 6.9 GPa (1000 ksi). For efficiency of testing in these element testers, it is recommended that maximum Hertz stresses between 4.83 to 5.52 GPa (700 to 800 ksi) be used.

With maximum compressive stresses of less than 4.14 GPa (600 ksi), gross plastic deformation of rolling surfaces will generally not occur for normal hardened bearing steels (Ref. 14). However, Drutowski and Mikus (Ref. 15) reported that small amounts of plastic deformation can occur at maximum Hertz stresses as low as 1.1 GPa (160 ksi). Drutowski (Ref. 16) further reported that for AISI 52100 steel there was an inversion between hardness and the maximum Hertz stress necessary for the initiation of plastic deformation. For a Rockwell C hardness of 62, the onset of plastic deformation occurs at a maximum Hertz stress of 1.92 GPa (278 ksi). For a Rockwell C hardness of 58, the onset occurs at a maximum Hertz stress of 2.6 GPa (377 ksi). Drutowski (Ref. 16) concluded that the contact stress at which plastic deformation is initiated is a function of the steel structure, but is independent of the diameter of the rolling ball (roller).

Usually, in normal bearing operation, gross plastic deformation is of no concern. However, in laboratory fatigue tests of rolling elements, stresses greater than 4.14 GPa (600 ksi) are the rule rather than the exception. Due to the isotropic or kinematic hardening the gross plastic deformation is accompanied by changes in the contact geometry, residual stresses and yield limit. As the amount of plastic deformation increases, the contact stress is reduced from that calculated using the Hertz formulas. It was found that the resultant Hertz stress is not only affected by the applied load, material hardness and structure but also by the elastohydrodynamic film formed (Ref. 14).

Figure 4(a) is a schematic diagram of the transverse section of a ball surface or crowned roller. The line of the true sphere or crown and the profile after plastic deformation and wear are shown. Figure 4(b) is a schematic diagram of a surface trace of a transverse section with deviations from that of the true sphere highly magnified (Ref. 17).
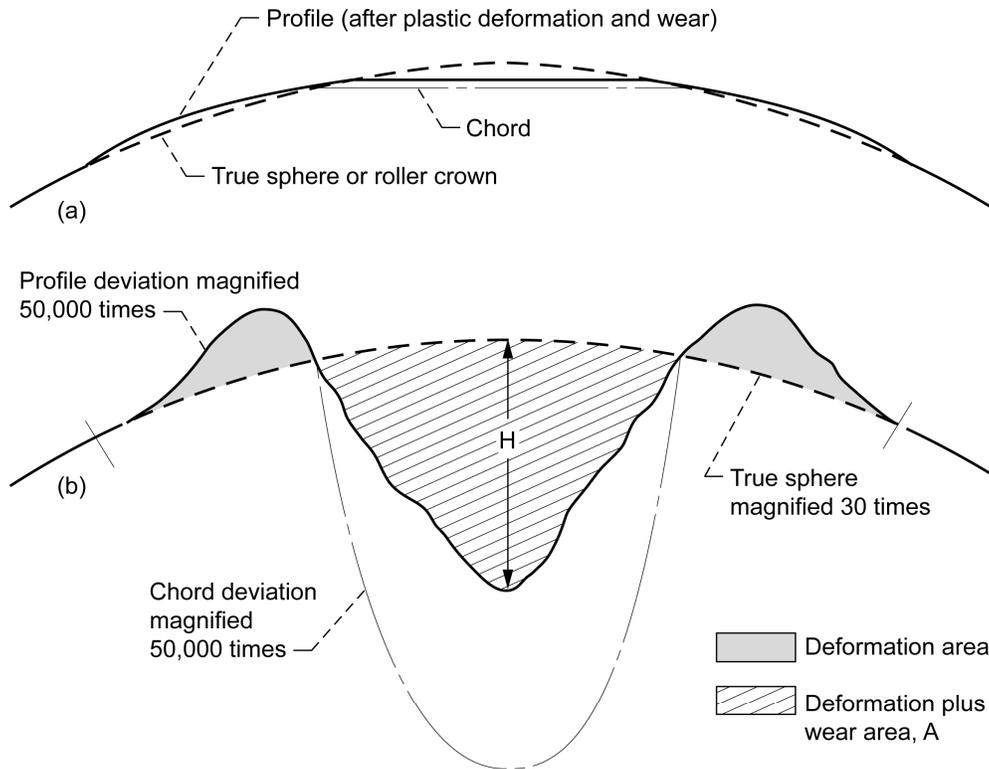
Figure 4.—Cross section of stressed ball track (not to scale) (Ref. 17). (a) Schematic diagram of transverse section of ball surface. (b) Schematic diagram of surface trace of transverse section with deviation from true sphere or roller crown highly magnified.

For many applications where gross plastic deformation occurs, it is necessary to calculate the effective Hertz stress or the contact stress after plastic deformation occurs (Ref. 18). This can be accomplished by deriving the radius of curvature R_p of the deformed rolling element as shown in Appendix A. Referring to Figure 5(a), for a convex surface such as a ball or a crowned roller,

$$R_p = \frac{\left(\dfrac{A}{H}\right)^2}{2\left\{ R - \left[R^2 - \left(\dfrac{A}{H}\right)^2 \right]^{1/2} - H \right\}} \tag{1}$$

The deformed radius R_p' (not shown) in the plane perpendicular to the plane of the profile shown in Figure 5(a) is

$$R_p' = R' - H \tag{2}$$

Where R' is the radius of the body in the perpendicular plane. Since H is extremely small relative to R;

$$R_p' = R' \tag{3}$$

Substituting R_p into the Hertz equations for contact stress, the effective Hertz stress after gross plastic deformation of the rolling–element surface can be calculated.
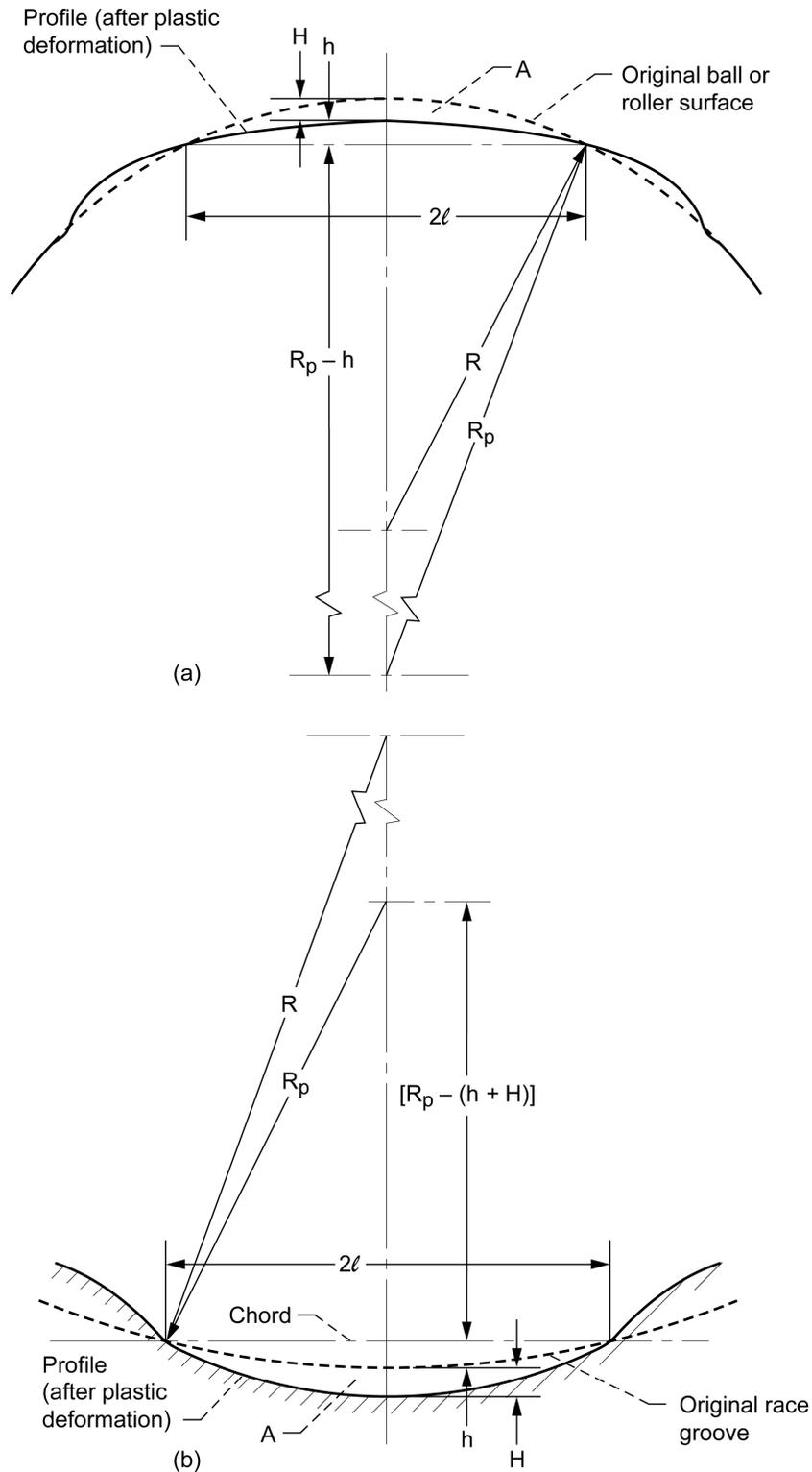
Figure 5.—Rolling-element bearing surfaces after plastic deformation (Ref. 17).
(a) Cross sectional of ball or crowned roller surface (see Fig. 4). (b) Cross
sectional of race surface.

For a race groove surface having a concave or negative radius R, as shown in Figure 5(b),

$$R_p = \frac{\left(\dfrac{A}{H}\right)^2}{2\left\{ R - \left[R^2 - \left(\dfrac{A}{H}\right)^2 \right]^{1/2} + H \right\}}$$ (4)

The area of deformation (and wear) A and the track depth H can be measured directly from a surface contour trace. Because plastic deformation can hardly change the roller diameter, the modified radius of curvature R_p as derived should only be applied to ball bearings, not to cylindrical roller bearing.

The effect of deformation and wear on the profile radius and the resultant maximum Hertz stress is illustrated in Table 1 for the NASA Five-Ball Fatigue Tester. The radius of curvature across the running track of the upper test ball is increased. Only considering deformation of the upper test ball, the resultant maximum Hertz stress is decreased by approximately 5 percent. However, considering deformation of both the upper and lower balls, the maximum Hertz stress is decreased by approximately 10 percent (Ref. 18). At an initial maximum Hertz stress of approximately 4.14 GPa (600 ksi) no plastic deformation was measured. This stress reasonably correlates with those stresses reported in the ISO Standards (Ref. 19) of 4.2 (609 ksi) and 4.0 GPa (580 ksi) related to the static load capacity of ball and roller bearings, respectively.

TABLE 1.—DEFORMATION AND WEAR AND THEIR EFFECT ON MAXIMUM HERTZ STRESS FOR AISI M–50
STEEL BALLS IN NASA FIVE-BALL FATIGUE TESTER
[Ball dia., 12.7×10^{-3} m (0.500 in.); Rockwell C hardness, 62; initial maximum Hertz stress, 5.52 GPa (800 ksi); contact angle, 10°; number of stress cycles, 30×10^3) (data from (Ref. 17)).]

Lubricant type	Lubricant designation	Original profile Radius, R, m (in.)	Deformation and wear area from surface trace, A (Fig. 4), m² (in.²)	Depth from original profile to deformed profile, H, (Figs. 4 and 5(a)), m (in.)	Calculated profile radius, Rp (Fig. 5(a)), (from Eq. (1)), m (in.)	Effective maximum Hertz stress, GPa (ksi)	
						No deformation and wear of support balls assumed	Deformation and wear of support balls assumed equal to test ball
Ester	NA–XL–3	6.35×10^{-3} (0.250)	4.95×10^{-10} (7.67×10^{-7})	16.68×10^{-7} (6.567×10^{-5})	8.35×10^{-3} (0.329)	5.27 (765)	5.03 (730)
	NA–XL–8	6.35×10^{-3} (0.250)	5.16×10^{-10} (8.00×10^{-7})	16.75×10^{-7} (6.596×10^{-5})	8.18×10^{-3} (0.322)	5.29 (767)	5.06 (734)
Mineral oil	NA–XL–4	6.35×10^{-3} (0.250)	6.13×10^{-10} (9.50×10^{-7})	20.19×10^{-7} (7.947×10^{-5})	8.79×10^{-3} (0.346)	5.23 (759)	4.95 (718)
	NA–XL–7	6.35×10^{-3} (0.250)	5.37×10^{-10} (8.33×10^{-7})	17.95×10^{-7} (7.067×10^{-5})	8.51×10^{-3} (0.335)	5.27 (763)	5.00 (725)

The contact model is presented as an introduction to the topic, and can be used with reasonable engineering certainty to determine the reduction in the contact stress resulting from gross plastic deformation. However, for greater accuracy, recent additional work in elasto-plastic point contacts was reported on by Chen et al. (Ref. 20). Nelias et al. (Refs. 21 and 22) have reported on elastic-plastic sliding contacts, and Wang et al. (Ref. 23) have modeled elastic-plastic contacts between a sphere and a flat.

Full-Scale Bearing Testers

As discussed above, the use of rolling-element fatigue testers qualitatively compare with results of full-scale bearing tests and/or from field data. However, the variables once defined from bench type tests must be subject to realistic operating conditions such as magnitude and type of load, speed, mode of lubrication and temperature such as those found in actual bearing applications (Ref. 24). In general, for fatigue testing full-scale bearings it is recommended that maximum resultant Hertz stresses be equal to or less than 2.41 GPa (350 ksi). However, maximum Hertz stresses as high as 3.1 GPa (450 ksi) can be used for testing many types of bearings. These requirements were discussed by A.T. Galbato (Ref. 24). He appropriately stated that, "*The combined influence of important environmental conditions which simulate as closely as possible the expected service environment and that a sufficient number of tests be performed to evaluate the scatter of fatigue life as characterized by the Weibull distribution* (function) (Ref. 24)."

From Galbato (Ref. 24), the various arrangements for arranging testing ball and roller bearings are illustrated in Figure 6. "*The standard bearing test rigs include a stationary frame, a movable housing frame, and a single test shaft on which test bearings are mounted. The type and size of the bearing will determine the overall size of the test rig and drive system. Operating conditions include the magnitude and type of load, speed, mode of lubrication and temperature.*" These variables should be continuously monitored.
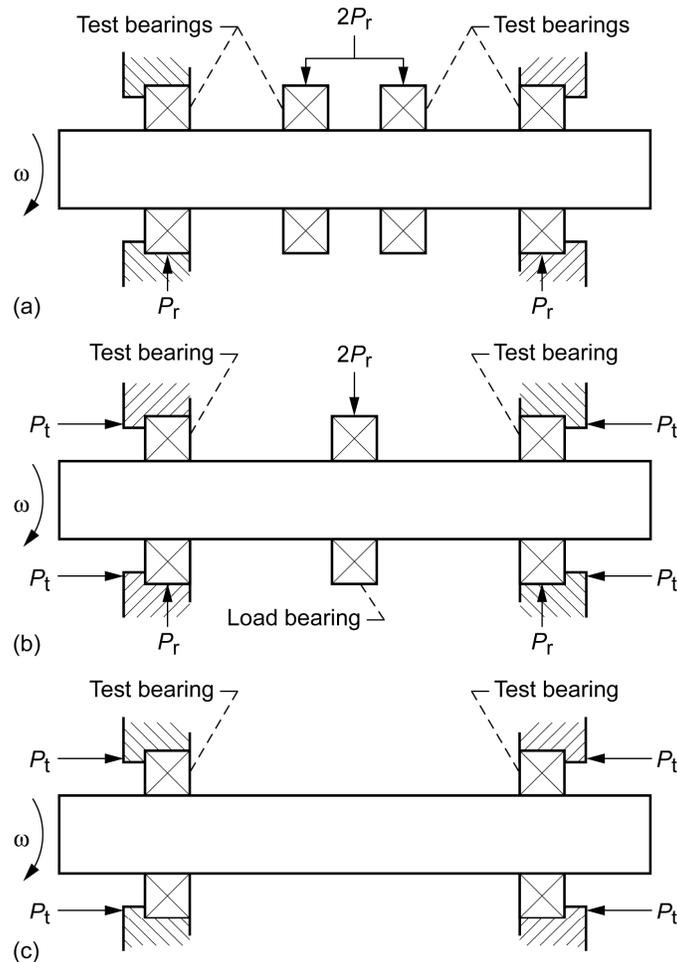

Figure 6.—Basic configurations for standard rolling-element bearing test rigs including stationary frame movable housing frame and single test shaft for mounted bearings (from Galbato (Ref. 24)). (a) Four-bearing arrangement for radial loading only. (b) Three-bearing arrangement for combined loading. (c) Two-bearing arrangement for thrust loading only.

A four bearing configuration for radial only loading is shown in Figure 6(a) (Ref. 24). This arrangement permits simultaneous testing of four bearings. The applied radial load (2P) acts on the two inboard bearings. The reactionary forces (P) act on the two inboard bearings.

A three-bearing configuration for combined loading is shown in Figure 6(b) (Ref. 24). This arrangement provides for the combined loading of the two outboard bearings. The applied load (2P) acts on the center load radial bearing (B). The thrust load (T) is applied axially on one outboard bearing and reacted to by the other. In this arrangement, the reactionary radial load (P), in combination with the applied and reactionary thrust load (T) acting on the outboard test bearings, provides a simultaneous combined loading on these two bearings (Ref. 24).

A two bearing configuration for thrust loading only is shown in Figure 6(c). In this arrangement, the thrust load (T) is applied axially to one bearing and is reacted to by the second bearing.

The lubrication mode for these type tests is usually recirculating oil jet lubrication. Oil filtration of 10 μm or better should be provided and the filter replaced after each test. Other lubrication modes that are used are under- and through-the-race lubrication and oil mist. While oil bath lubrication can be used for low speed tests, it is not recommended. It is recommended that the oil condition be monitored and that the oil be changed after each test. The used oil should be discarded and not reused. A sample of oil from each test should be saved and cataloged for later analysis, if necessary. In either case, the same lubrication conditions have to be assured in the most loaded areas for all four bearings, especially when bath lubrication is used.

Automatic shut-off systems are used for each test rig based on temperature rise and monitoring any vibration amplitude increase that indicates the occurrence of an incipient fatigue spall. The bearings' oil-in and out temperatures and the bearings' outer- (and, if possible, inner-) ring temperatures are measured and monitored. Lubricant flow is measured and monitored. Chip detectors in the lubricating system should be critically placed to detect a metallic chip of a significant size emerging from a spall. Time of operation should be monitored for each test machine and each test bearing (Ref. 24).

Procedures for Testing Full-Scale Bearings

It should again be emphasized that bench-type testing is used to observe comparative trends due to changes in lubricant, material type, material processing, operating parameters, etc. While great efforts are made to appropriately select and control testing technique and test parameters the only way to obtain quantitative data is to test full-scale bearings. However, the cost of testing bearings can be more than 100 times greater than simplified rolling-element specimens. Similar caution and test procedures should be taken with full-scale bearings as with bench type testers discussed above.

A common problem in testing full-scale bearings is misalignment of the bearing within the rig. Prior to test, the bearing should be measured for dimensional clearances and tolerances. In general, test stresses lower than 2.41 GPa (350 ksi) maximum Hertz are suggested. However, maximum Hertz stresses as high as 3.1 GPa (450 ksi) on the inner race can be used for testing many types of bearings.

Another common problem associated with full-scale bearing testing is the failure of investigators to consider or report the interference fits between the bearing bore and shaft and the bearing outer diameter and housing. The interference fit between the bearing bore and the shaft will induce tensile hoop stresses in the bearing inner race. These tensile stresses can increase the magnitude of shearing stresses below the contacting surface between the rolling elements and the bearing inner race and reduce the bearing fatigue life (Refs. 25, 26, and 27).

The interference fit between the bearing bore and shaft in combination with the interference fit between the bearing outer diameter and the housing will reduce the bearing's internal clearance and affect the bearing fatigue life. Hence, the same bearing run under extensively the same operating conditions can produce significantly different life results because of interference fits. Accordingly, a "fit-up study" should be conducted and reported regarding the effect of interference fit and bearing internal clearance. Detailed findings and insights regarding interference fit can be found in Coe and Zaretsky (Ref. 25) and Oswald et al. (Refs. 26 and 27).

Another problem to be alerted to is that the static load capacity of the bearing should not be exceeded. This is the maximum load that a bearing can be permitted to support when not rotating. It is arbitrarily defined as the load that will produce a permanent indentation of the race having a depth equal to 0.0001 times the rolling-element diameter. Based upon ISO Standard ISO 76:2006 (Ref. 19) for through hardened bearing steel of hardness Rockwell C 58 and above, this load correlates to a maximum Hertz stress of approximately 4.0 GPa (580 ksi) for cylindrical roller bearings. For ball bearings this load correlates to a maximum Hertz stress of approximately 4.2 (609 ksi) (Ref. 19). When permanent deformation exceeds this value, bearing vibration and noise can noticeably increase when the bearing is subsequently rotated under lesser loads.

Although it is not recommended, a bearing can be loaded above the static load capacity as long as the load is applied when the bearing is rotated. For an angular-contact ball bearing, the plastic deformation that occurs during rotation will be distributed evenly around the periphery of the races and will not be harmful until it becomes more extensive. However, for a radially loaded ball or roller bearing, when the maximum Hertz stress on the outer race exceeds 4.0 GPa (580 ksi), the plastic deformation will be concentrated at the position of the maximum loaded rolling element. In this event, exceeding the bearing's static load capacity would be unacceptable.

In many applications where marginal lubrication is a factor, such as at elevated temperature, high-surface tangential speeds are desirable in the bearings because of elastohydrodynamic effects. This can make a difference between the bearing operating for relatively short time periods with wear and surface distress being the failure mode or operating for extended time periods with rolling-element fatigue being the failure mode. Lower speeds will not necessarily give longer lives in terms of inner-race revolutions or conversely, higher speeds will not give shorter lives in terms of actual running time. Temperatures should be monitored on the inner race, the outer race and in the housing around the bearing. Lubricant sump and ambient temperatures should also be monitored.

Post test examination of the failed test bearings should record those components, i.e., balls or rollers, inner and outer races, of each bearing that has failed and their respective failure mode. Based on the methods of Johnson (Ref. 10), it is possible to not only determine the statistical life and failure distribution of the bearing group but also the lives of the ball or roller set, the inner race and the outer race.

Correlation of Bench-Type Tests With Full-Scale Bearing Results

Bench-type fatigue tests can qualitatively rank material, lubricant, or operating variables. This is illustrated in Figure 7, which is a comparison of the relative dynamic load capacity obtained in the NASA Five-Ball Fatigue Tester with four different test lubricants at 149 °C (300 °F) to fatigue tests with 7208-size deep-groove ball bearings with the same four test lubricants (Ref. 17). Each test lubricant for the bench tests and the full-scale bearing tests came from a single batch. While the operating conditions, bearing steels and contact geometries between the bench test rig configuration and the full-scale bearings are different, both type of tests ranked the fatigue lives with each of the four lubricants in the same order. These data are summarized in Table 2.

The operating conditions of the bench-type tests typically differ from the in-service operating conditions for full-scale rolling-element bearings. Most bench-type tests are accelerated tests with extreme conditions (higher speeds, higher loads, and/or higher operating temperatures) as compared to typical bearing operating conditions. While there may be differences in the magnitude of the quantitative lives, the general trends are comparable, that is, there is agreement in relative rankings of materials, lubricants, operating conditions, etc.
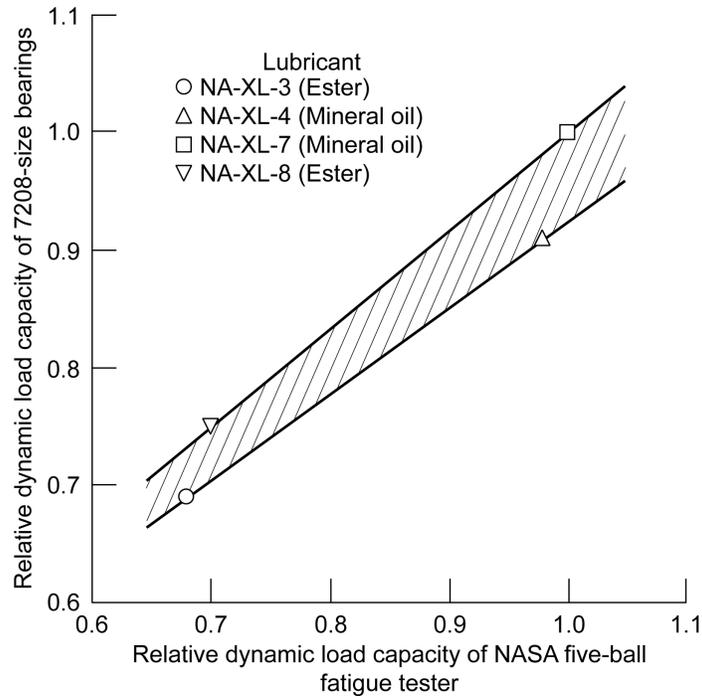
Figure 7.—Relative dynamic load capacity of 7208-size bearings
as function of relative dynamic load capacity of five-ball fatigue
tester for various lubricants at 149 °C (300 °F) (Ref. 17).

TABLE 2.—COMPARISON OF ROLLING-ELEMENT FATIGUE LIVES
OBTAINED WITH FOUR TEST LUBRICANTS IN NASA FIVE-BALL FATIGUE
TESTER AND 7208-SIZE ANGULAR-CONTACT BALL BEARINGS (REF. 17)

Lubricant type	Lubricant designation	Five-ball fatigue tester[a]		7208-size angular-contact ball bearings[b]	
		L_{10} life, millions of stress cycles	Ratio of L_{10} life to L_{10} life with NA–XL–7	L_{10} life, millions of inner-race revolutions	Ratio of L_{10} life to L_{10} life with NA–XL–7
Ester	NA–XL–3	13.7	0.31	1.1	0.33
	NA–XL–8	14.9	0.34	1.4	0.42
Mineral oil	NA–XL–4	42.5	0.96	2.5	0.76
	NA–XL–7	44.5	1.00	3.3	1.00

[a]Temperature, 149 °C (300 °F); maximum Hertz stress, 5.52 GPa (800 ksi); material,
vacuum processed (VP) AISI M–1 steel; steel Rockwell C hardness, 63; speed,
10,000 rpm.
[b]Temperature, 149 °C (300 °F); thrust load, 20,461 N (4,600 lb); maximum Hertz stress,
2.41 GPa (350 ksi); materials (assumed to be) air-melt processed (AM)
AISI 52100 steel; hardness, not reported; speed, 3,450 rpm.

Figure 8 compares the relative load capacity also obtained in the NASA Five-Ball Fatigue Tester to the load capacity of 207-size deep-groove ball bearings where ball hardness is the variable (Ref. 28). As can be seen for the lubricant and hardness variables, the correlation of the Five-Ball Fatigue Tester results with those of full-scale bearing tests on a relative basis is excellent. For both sizes of bearings, the maximum stress level was approximately 2.41 GPa (350 ksi) at the inner race-ball contact in comparison with 5.52 GPa (800 ksi) for the five-ball tester.
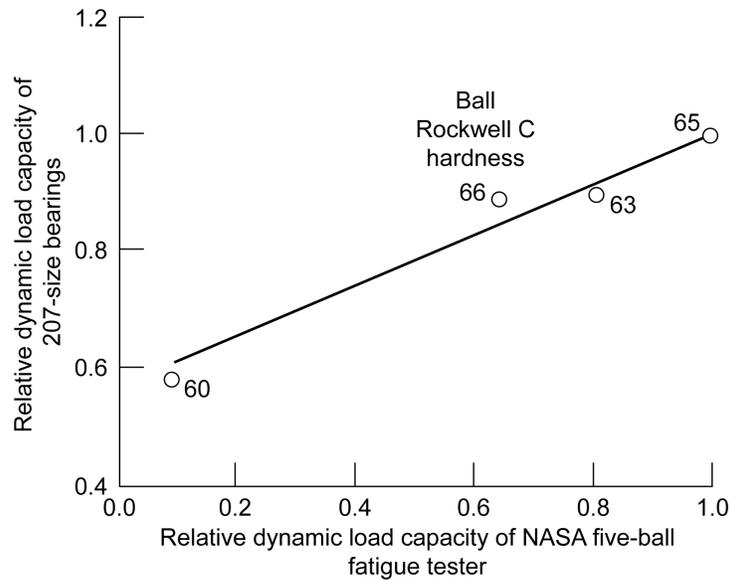
Figure 8.—Relative dynamic load capacity of 207-size bearings as function of relative dynamic load capacity of five-ball fatigue tester for various dynamic load ball hadrness. Nominal hardness of upper ball (for five-ball tests) and inner race (for bearings), 63 Rockwell C (Ref. 28).
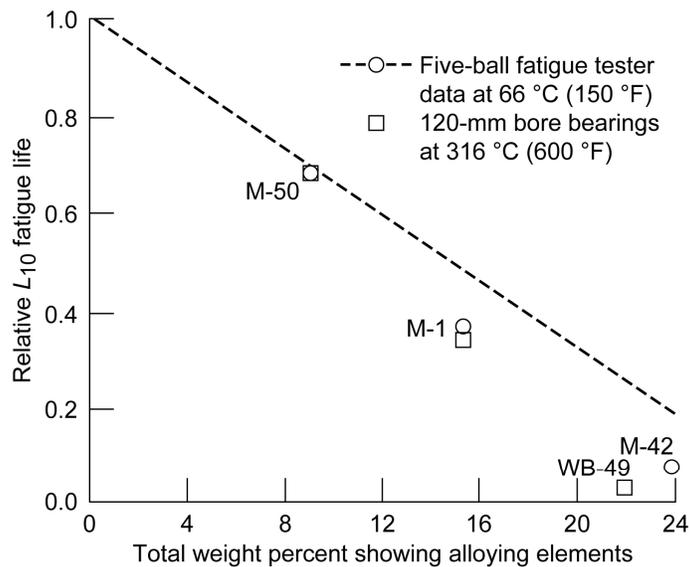

Figure 9.—Comparison of results from NASA five-ball fatigue tester and 120-mm bore angular-contact ball bearings showing effect of total weight percent of alloying elements on fatigue life (Ref. 29).

A third example of the correlation between the NASA Five-Ball Fatigue Tester and full-scale bearings is shown in Figure 9 (Refs. 29 and 30). The relative L_{10} lives of bearings made from three steels are compared to rolling-element fatigue data from the NASA Five-Ball Fatigue Tester. These data show the effect of total percent weight of alloying element on bearing life. The bearings were thrust loaded 120-mm bore angular-contact ball bearings made from AISI M-1, AISI M-50, and WB-49 steels (Ref. 30). The AISI M-42 steel run in the five-ball tester had a similar microstructure to WB-49. Both

steels contained relative high percentages of cobalt. The bearings were run at a maximum Hertz stress at the inner race of 2.23 GPa (323 ksi) and a temperature at the outer ring of 316 °C (600 °F). The five-ball tests were run at a nominal temperature of 66 °C (150 °F). Again, there is excellent correlation between the NASA Five-Ball Fatigue Tester fatigue data with the full-scale bearing fatigue data.

These comparisons show that bench-type fatigue testers can reliably identify qualitative effects of many variables on rolling-element fatigue life. By bench marking these life results to an already existing data base, it is possible to develop bearing life modifying factors with the Lundberg-Palmgren theory (Ref. 31) to predict bearing life with reasonable engineering certainty (Ref. 1).

Testing Methodologies That Reduce Total Test Time

Experimentally determining rolling-element bearing life is a complex, time- consuming, and costly task. In addition to the driving need to find methods to reduce testing time (and cost), not all bearing and/or specimens that are tested will or can be expected to fail in a reasonably, prescribed time limit. Thus, methods to reduce testing time are of great importance. An early explanation of three methodologies for reducing testing time can be found in the classic work of Leonard G. Johnson (Ref. 10). In the first method, more specimens are run simultaneously than are intended to fail. For example, for a Weibull slope of 1.0, the median time to fail 10 out of 20 samples is 76 percent less than the median time required to fail 10 out of 10 samples. This is assuming that there are no replacements of failed specimens, all testers are the same, and all specimens are run simultaneously. Since the width of the confidence band is determined by the number of items failed and not the total number of specimens in a test (Ref. 10), the number failed is 10 in both cases. As a result, the only difference is that the 10 items having the lowest lives in a lot of 20 are plotted on a Weibull plot instead of all 10 specimens in a lot of 10 (Ref. 10). The first scenario will take 24 percent of the time it takes for the second, and yet the necessary life information can be obtained by the first case.

Sequential analysis is a second methodology for shortening total test time described by Johnson (Ref. 10). Test specimens are failed sequentially one after the other. The total number of specimens needed to fail is not known in advance. The investigator decides after each failure whether or not additional testing is required. In this manner, the bare minimum number of runs needed to demonstrate an improvement or worsening of life is conducted. A method similar to this has been used extensively by E.V. Zaretsky and colleagues since the late 1950s. An estimate of the 50-percent life (L_{50}) is made and test bearings are then run on identical testers until this life is reached. As samples fail or are suspended at the L_{50} life, they are removed, and new samples are mounted and evaluated to the estimated L_{50}. In this manner, at least 50 percent of the samples are typically failed out of the entire available population. In some cases, the L_{50} target may have to be adjusted as dictated by the number of failures encountered. The experimenter decides after each failure whether or not additional testing is required. In this manner, the minimum number of runs needed to demonstrate an improvement or worsening of life is conducted.

Sudden death testing (SDT) is the third method of reducing testing time described by Johnson (Ref. 10). The total accumulated test time is reduced by not running all specimens to failure. The total number of specimens to be evaluated n is divided into equal-sized subgroups according to the number of available experimental testers. Thus, there are m specimens in each equal-sized subgroup, and there are a total of r subgroups. The total number of specimens n equal m times r. The specimens in each subgroup are fatigue tested identically and simultaneously on different testers. The first subgroup of specimens is run until the first failure occurs. At this point, the surviving specimens are suspended and removed from testing. An equal set of new specimens numbering m samples is next tested until the first failure in that subpopulation. This process is repeated until one failure is generated for each of the subgroups. In the end, r failures are generated while $(m-1) \times r$ samples are suspended. Thus, the total accumulative test time is the time to fail r specimen times the number of samples concurrently tested m, not the time for n failures. With proper corrections and analysis (Johnson (Ref. 8)), reliability of the life predicted by this sudden death methodology from r failures is comparable to that obtained when failing the entire population. A detailed description of sudden death testing (SDT) is given in Appendix B.

Proving that any of these methodologies reduces total test time while predicting accurate bearing fatigue lives would require the generation of a significant and unreasonable quantity of experimental data. Vlcek, Hendricks, and Zaretsky (Ref. 32) have shown that computer modeling of bearing life based upon Weibull-Johnson Monte Carlo simulations results in reasonable engineering predictions of bearing life that are relatively easy to determine. Vlcek, et al. (Ref. 33) also performed Monte Carlo simulations combined with sudden death testing in order to compare resultant bearing lives to calculated bearing life and the cumulative test time and calendar time relative to sequential and censored sequential testing. Reductions up to 40 percent in bearing test time and calendar time can be achieved by testing to failure or the L_{50} life and terminating all testing when the last of the predetermined bearing failures has occurred. Vlcek, Hendricks, and Zaretsky found that sudden death testing is not a more efficient method to reduce bearing test time or calendar time when compared to censored sequential testing (Ref. 33).

Fatigue Data Analysis

Weibull Distribution Function

In 1939, W. Weibull (Refs. 8 and 9) developed a method and an equation for statistically evaluating the fracture strength of materials based upon small population sizes. This method can be and has been applied to analyze, determine, and predict the cumulative statistical distribution of fatigue failure or any other phenomenon or physical characteristic that manifests a statistical distribution. The dispersion in life for a group of homogeneous test specimens can be expressed by

$$\ln\ln\frac{1}{S} = e\ln\left(\frac{L - L_\mu}{L_\beta - L_\mu}\right) \quad \text{where} \quad 0 < L < \infty;\ 0 < S < 1 \tag{5}$$

where S is the probability of survival as a fraction ($0 \le S \le 1$); e is the slope of the Weibull plot; L is the life cycle (stress cycles); L_μ is the location parameter, or the time (cycles) below which no failure occurs; and L_β is the characteristic life (stress cycles). The characteristic life is that time at which 63.2 percent of a population will fail, or 36.8 percent will survive.

The format of Equation (5) is referred to as a three-parameter Weibull analysis. For most—if not all—failure phenomenon, there is a finite time period under operating conditions when no failure will occur. In other words, there is zero probability of failure, or a 100-percent probability of survival, for a period of time during which the probability density function is nonnegative. This value is represented by the location parameter L_μ. Without a significantly large data base, this value is difficult to determine with reasonable engineering or statistical certainty. As a result, L_μ is usually assumed to be zero and Equation (5) can be written as

$$\ln\ln\frac{1}{S} = e\ln\left(\frac{L}{L_\beta}\right) \quad \text{where } 0 < L < \infty;\ 0 < S < 1 \tag{6}$$

This format is referred to as the two-parameter Weibull distribution function. The estimated values of the Weibull slope e and L_β for the two-parameter Weibull analysis may not be equal to those of the three-parameter analysis. As a result, for a given survivability value S, the corresponding value of life **L** will be similar but not necessarily the same in each analysis.

By plotting the ordinate scale as ln ln($1/S$) and the abscissa scale as ln L, a Weibull cumulative distribution will plot as a straight line, which is called a "Weibull plot." Usually, the ordinate is graduated in statistical percent of specimens failed F where $F = [(1 - S) \times 100]$. Figure 10(a) is a generic Weibull plot with some of the values of interest indicated. Figure 10(b) is a Weibull plot of actual bearing fatigue data.
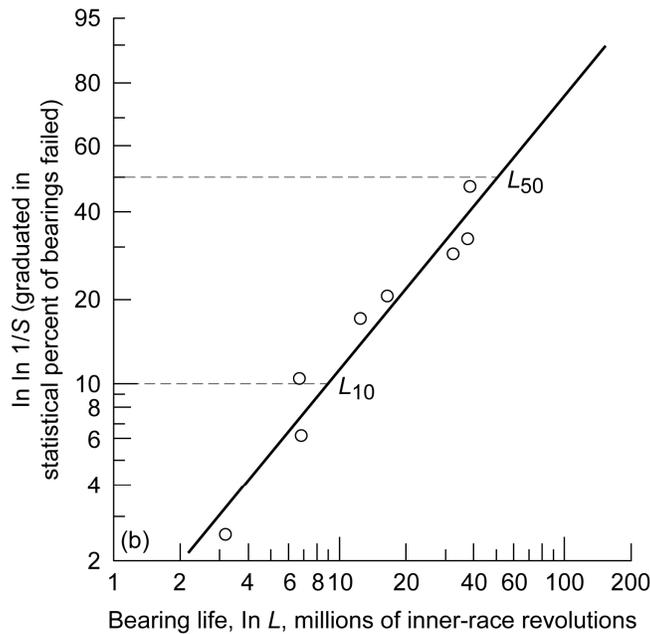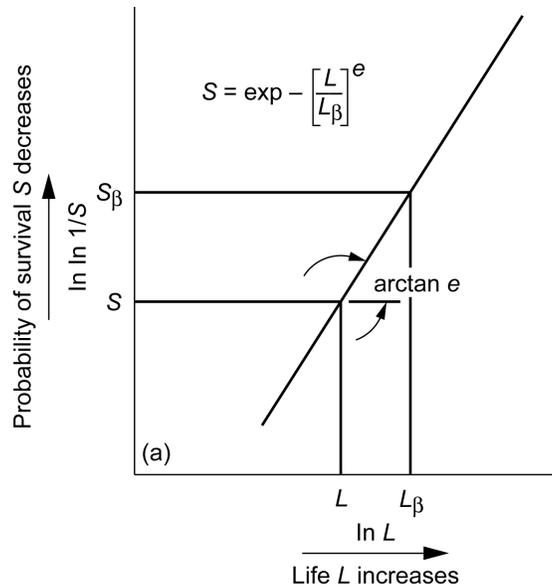
Figure 10.—Weibull plot where (Weibull) slope or tangent of line is e; probability of survival, S_β, is 36.8 percent at which $L = L_\beta$, or $L/L_\beta = 1$. (a) Schematic. (b) Rolling-element bearing fatigue data.

The Weibull plot can be used to evaluate any phenomenon that results in a statistical distribution. The tangent of the resulting plot, called the "Weibull slope" and designated by e, defines the statistical distribution. Weibull slopes of 1, 2, and 3.57 represent exponential, Rayleigh, and Gaussian (normal) distributions, respectively.

The scatter in the data is inversely proportional to the Weibull slope; that is, the lower the value of the Weibull slope, the larger the scatter in the data, and vice versa. The Weibull slope is also liable to statistical variation depending on the sample size (data base) making up the distribution (Ref. 10). As the sample size becomes smaller, there is a greater statistical variation in the Weibull slope.

Whether the data is generated experimentally or simulated analytically, the ultimate goal is to determine the life and characteristics of a larger population from a limited amount of data. There are various statistical methods for determining bearing life estimates from fatigue data that for practical engineering purposes, give similar results. These methods differ significantly; however, in their level of complexity to apply and limitations to their application. For its relative ease of use and engineering application with comparable reliability, we have selected the Weibull-based Leonard G. Johnson approach (Ref. 10) which utilizes a linear regression least-square-fit method over the significantly more complicated maximum likelihood estimation method (Ref. 34). Experience of the authors' has been that least-square-fit method of Johnson (Ref. 10) gives similar results to that of the maximum likelihood estimation methods (Refs. 34 and 35). However, the maximum likelihood estimation method is more sensitive to early failures, biasing the Weibull slope to indicate more scatter than actually exists in the data. There are computer programs that are commercially available that can perform these Weibull analyses.

Bearing Component Lives

Where there are design, manufacturing, material and metallurgical variables among the inner race, outer race and rolling-element (ball or roller) set, it is important to distinguish the effects of these variables on the resultant life of a rolling-element bearing. Lundberg and Palmgren (Ref. 31) present bearing life as only a function of the lives of the inner and outer races as follows:

$$\left(\frac{1}{L_{10}}\right)^e = \left(\frac{1}{L_{ir}}\right)^e + \left(\frac{1}{L_{or}}\right)^e \tag{7a}$$

They do not directly calculate the life of the rolling-element (ball or roller) set of the bearing. However, through benchmarking of the equations with bearing life data by use of a material-geometry factor, the life of the rolling-element set is implicitly included in the bearing life calculation. The material-geometry factor does not differentiate the effects of these variables but empirically blends them together. Accordingly, Lundberg and Palmgren (Ref. 30) should have written their equation relating bearing life to the individual components lives based on the Weibull equation (Refs. 8 and 9) as follows:

$$\left(\frac{1}{L_{10}}\right)^e = \left(\frac{1}{L_{ir}}\right)^e + \left(\frac{1}{L_{re}}\right)^e + \left(\frac{1}{L_{or}}\right)^e \tag{7b}$$

where the Weibull slope e is the same for each of the components as well as for the bearing as a system. The value of the L_{10} life is the same as that in Equation (7a). However, the values for the inner and outer race live will be greater than those of Equation (7a). Equations (7a) and (b) are based on strict series reliability derived in Appendix C. Equation (7b) can be rewritten as

$$1 = \left[\frac{L_{10}}{L_{ir}}\right]^e + \left[\frac{L_{10}}{L_{re}}\right]^e + \left[\frac{L_{10}}{L_{or}}\right]^e \tag{7c}$$

While the experimental bearing L_{10} life may equal or greater than that calculated according to Lundberg and Palmgren (Ref. 31), the experimental values of the inner and outer race lives should always be higher than that calculated.

From Johnson (Ref. 10), the fraction of failures due to the failure of a bearing component is

$$\text{Fraction of inner-race failures} = \left[\frac{L_{10}}{L_{ir}}\right]^e \tag{8a}$$

$$\text{Fraction of rolling-element failures} = \left[\frac{L_{10}}{L_{re}}\right]^e \tag{8b}$$

$$\text{Fraction of outer-race failures} = \left[\frac{L_{10}}{L_{or}}\right]^e \tag{8c}$$

From Equations (8a) to (c), if the life of the bearing and the fractions of the total failures represented by the inner race, the outer race and the rolling-element set are known, the life of each of these components can be calculated. Hence, by observation, it is possible to determine the life of each of the bearing components with respect to the life of the bearing.

Bearing Life Variation

Vlcek et al. (Ref. 32) randomly assembled and tested 340 virtual bearing sets totaling 31,400 radially loaded and thrust-loaded rolling-element bearings. It was assumed that each bearing was assembled from three separate bins of components, with one bin containing 1000 inner rings; one with 1000 rolling element sets, and one with 1000 outer rings. The median ranks of the individual components were assigned and then virtual bearing assemblies were created using a Monte Carlo technique.

Vlcek et al. (Ref. 32) determined the L_{10} maximum limit and L_{10} minimum limit for the number of bearings failed, r, using a Weibull-based Monte Carlo method. By fitting the resultant lives for different size populations of failed bearings (Fig. 11), equations were determined for both of these limits:

$$\text{Maximum variation } L_{10} \text{ life} = \text{calculated } L_{10} \text{ life } (1+6r^{-0.6}) \tag{9a}$$

$$\text{Minimum variation } L_{10} \text{ life} = \text{calculated } L_{10} \text{ life } (1-1.5r^{-0.33}) \text{ where } r > 3 \tag{9b}$$

$$\text{Minimum } L_{10} \text{ life} = 0 \text{ where } r \leq 3 \tag{9c}$$

These curves compared favorably with the 90-percent confidence limits of Johnson (Ref. 10) at a Weibull slope of 1.5 (Fig. 12) (Ref. 32).

Moult (Ref. 6) published a series of successive fatigue tests with cylindrical roller bearings made from a single heat of air melted (AM) and subsequently consumable-electrode vacuum remelted (CVM) AISI 8620 steel conducted over a five year period. These bearings were lubricated with a single batch of Mil-L-7808 diester lubricant and three individual types of SAE 30 mineral oil lubricants. The base stocks of these mineral oils were a super-refined naphthenic, a naphthenic and a paraffinic. Moult's data base comprised approximately 106 roller bearing fatigue failures (Ref. 6). Individual test series ranged from 10 to 14 bearings with as many as 39 bearings making up a composite group used for purposes of comparison. The variation in Moult's data base varied in accordance with Equations (9a) to (c). For an example, the individual L_{10} lives for the air-melt (AM) AISI 8620 steel lubricated with the Mil-L-7808 lubricant varied from 85 to 1900 percent from the composite bearing L_{10} life value with this lubricant. Further, when comparing the variation in bearing L_{10} lives for the air-melt (AM) AISI 8620 steel lubricated with the Mil-L-7808 lubricant with the composite L_{10} bearing life obtained with the air-melt (AM) AISI 8620 steel bearings lubricated with the SAE 30 mineral oil, the bearing L_{10} lives with the Mil-L-7808 lubricant ranged from 7 to 115 percent of that obtained with the SAE 30 mineral oil (Ref. 6).
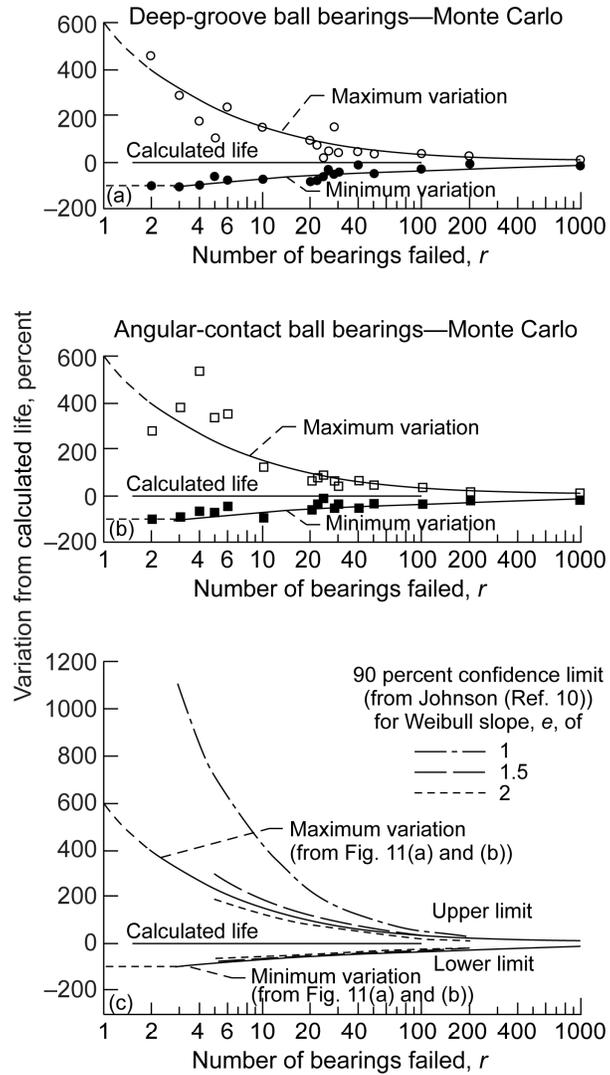
Figure 11.—Maximum and minimum variation of L_{10} lives as percent of calculated L_{10} for groups of r bearings and 90 percent confidence limits based on Weibull slope and number of bearings failed r (Ref. 32). (a) 50-mm-bore deep-groove ball bearing. (b) 50-mm-bore angular-contact ball bearing. (c) 90 percent confidence limits.
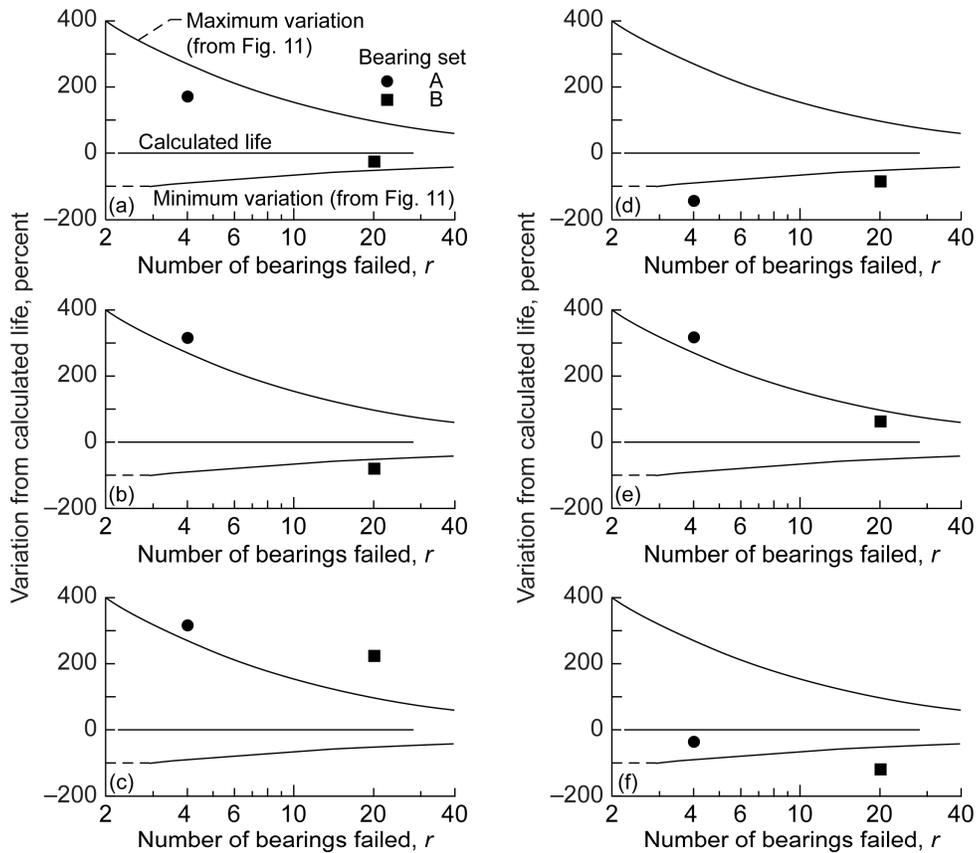
Figure 12.—Rules for comparing bearing life results to calculated life (Ref. 32).
(a) Bearing sets A and B are acceptable. (b) Bearing set A is acceptable. Bearing
set B is not acceptable. (c) Bearing sets A and B are acceptable. (d) Bearing sets
A and B are not acceptable. (e) Bearing sets A and B are acceptable. (f) Bearing
set A is acceptable. Bearing set B is not acceptable.

Rules can be implied from these results to compare and distinguish resultant lives of identical bearings either from two or more sources or made using different manufacturing methods. The following rules are suggested to determine if the bearings are acceptable for their intended application or if there are significant differences between the two groups of bearings.

1. If the L_{10} lives of both bearing tests are between the maximum and minimum L_{10} life variations, there can be no conclusion that there is a significant difference between the two sets of bearings regardless of the ratio of the L_{10} lives. The bearing sets are acceptable for their intended application (Fig. 12(a)).
2. If the L_{10} life of one set of bearings is greater than the maximum variation and the second set is less than the minimum value, there exists a significant difference between the bearing sets. Only one bearing set is acceptable for its intended application (Fig. 12(b)).
3. If the L_{10} lives of both sets of bearings exceed the maximum variation, the bearing life differences may or may not be significant and should be evaluated based upon calculation of confidence numbers according to the method of Johnson (Ref. 10). Both sets of bearings are acceptable for their intended application (Fig. 12(c)).
4. If the L_{10} lives of both sets of bearings are less than the minimum variation, the bearing life differences may or may not be significant. However, neither set of bearings is acceptable for its intended application (Fig. 12(d)).

5. If the L_{10} life of one set of bearings exceeds the maximum variation and the other set is between the maximum and minimum variation, the bearing life differences may or may not be significant and should be evaluated based upon calculation of confidence numbers according to the method of Johnson (Ref. 10). Both sets of bearings are acceptable for their intended application (Fig. 12(e)).
6. If the L_{10} life of one set of bearings is less than the minimum variation and the other set is between the maximum and minimum variation, there exists a significant difference between the bearing sets. Only one set of bearings is acceptable for its intended application (Fig. 12(f)).

Weibull Slope Variation

Johnson (Ref. 10) analyzed the probable variation of the Weibull slope as a function of the number of bearings tested to failure. Based on the Johnson analysis, in 90 percent of all possible cases the resultant Weibull slope will be within the limits shown in Figure 13 based upon a Weibull slope of 1.11. Based on Johnson, the approximate relation for the number of bearings failed r and the limits of the value of Weibull slope e equal to 1.11 are as follows:

$$\text{Maximum Weibull slope} = 1.11 + 1.31\ r^{-0.5} \tag{10a}$$

$$\text{Minimum Weibull slope} = 1.11 - 1.31\ r^{-0.5} \tag{10b}$$

The results of the extremes in the Weibull slopes for each group of the 10 bearing trials of r bearings from the Monte Carlo simulation of Vlcek, et al. (Ref. 33) are compared with the Johnson analysis (Ref. 10) in Figure 13.
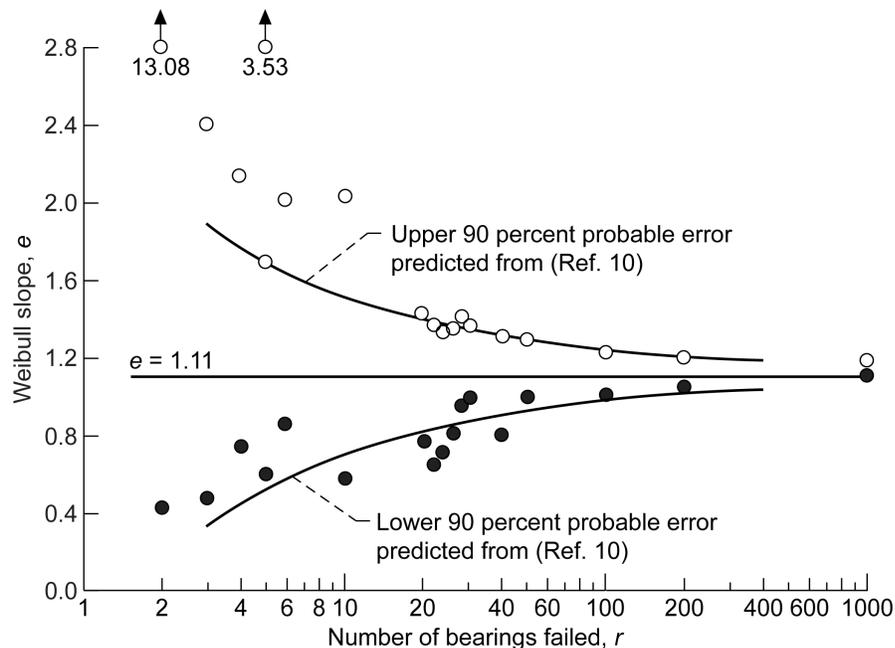

Figure 13.—Extremes of Weibull slope from Monte Carlo testing for each group of 10 bearing trials of r bearings compared with predicted 90 percent probable error (data from (Ref. 32)).

Confidence Number

It is important to know the confidence in the conclusions that can be derived from one series of tests relative to a standard test series. Johnson (Ref. 10) developed a statistical method for comparing two populations and/or variables that he termed "Confidence Numbers." For purposes of example, Weibull plots of lives of bearings made from two hypothetical bearing steels are compared in Figure 14. Lot 1 is made from a standard bearing steel containing 7 failures. Lot 2 is made from an experimental bearing steel and contains 10 failures. The L_{10} for Lots 1 and 2 are 38 and 76 hr, respectively. Both lots have a Weibull slope of 1.7. The question that can be asked is. "How much confidence can be placed in the apparent superiority of the experimental steel population (Lot 2) over the standard steel population (Lot 1)?"

In addition to the dependence upon the amount of separation between the two Weibull plots, or the ratio of the longer life to the shorter life at one level [F(x)], the answer to the question of confidence depends upon the number of failures (number of data points), r_1 and r_2 in each population of Lots 1 and 2, respectively, and also upon the Weibull slopes of their populations. An important point to be aware of is that the degree of confidence of one lot over the other need not be constant from one level [F(x)] to another. As an example, it is possible to have a significant improvement at the 50-percent life, L_{50}, without any improvement at the L_{10} life and vice versa. Since improvement in early life is of prime importance and is used for comparison purposes, the confidence in the L_{10} life will be considered. An extensive treatment was presented by Johnson (Ref. 10).

Johnson (Ref. 10) created a series of graphs shown in Figure 15 where 1/(1-C) is plotted against the L_{10} life ratio on logarithmic coordinates with the Weibull slope and $[(r_1 - 1)(r_2 - 1)]$ held constant. The graphs shown in Figure 15 are straight lines (or very nearly so). For convenience, the ordinate is graduated as the confidence number. Johnson (Ref. 10) claims no theoretical basis for the linearity of the plots.
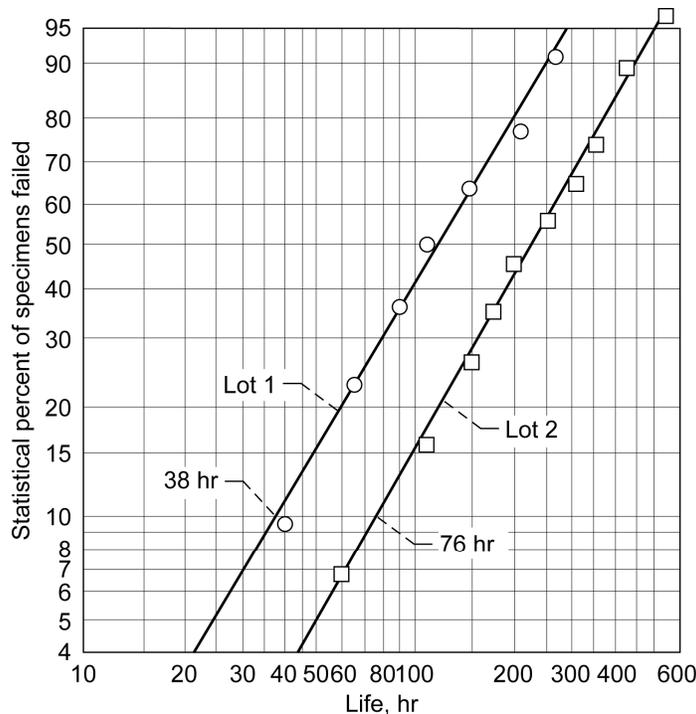

Figure 14.—Comparison of endurance test results for two material lots using Weibull plots. Ratio of L_{10} lives, 2; Weibull slope for each lot, 1.7 (Ref. 10).
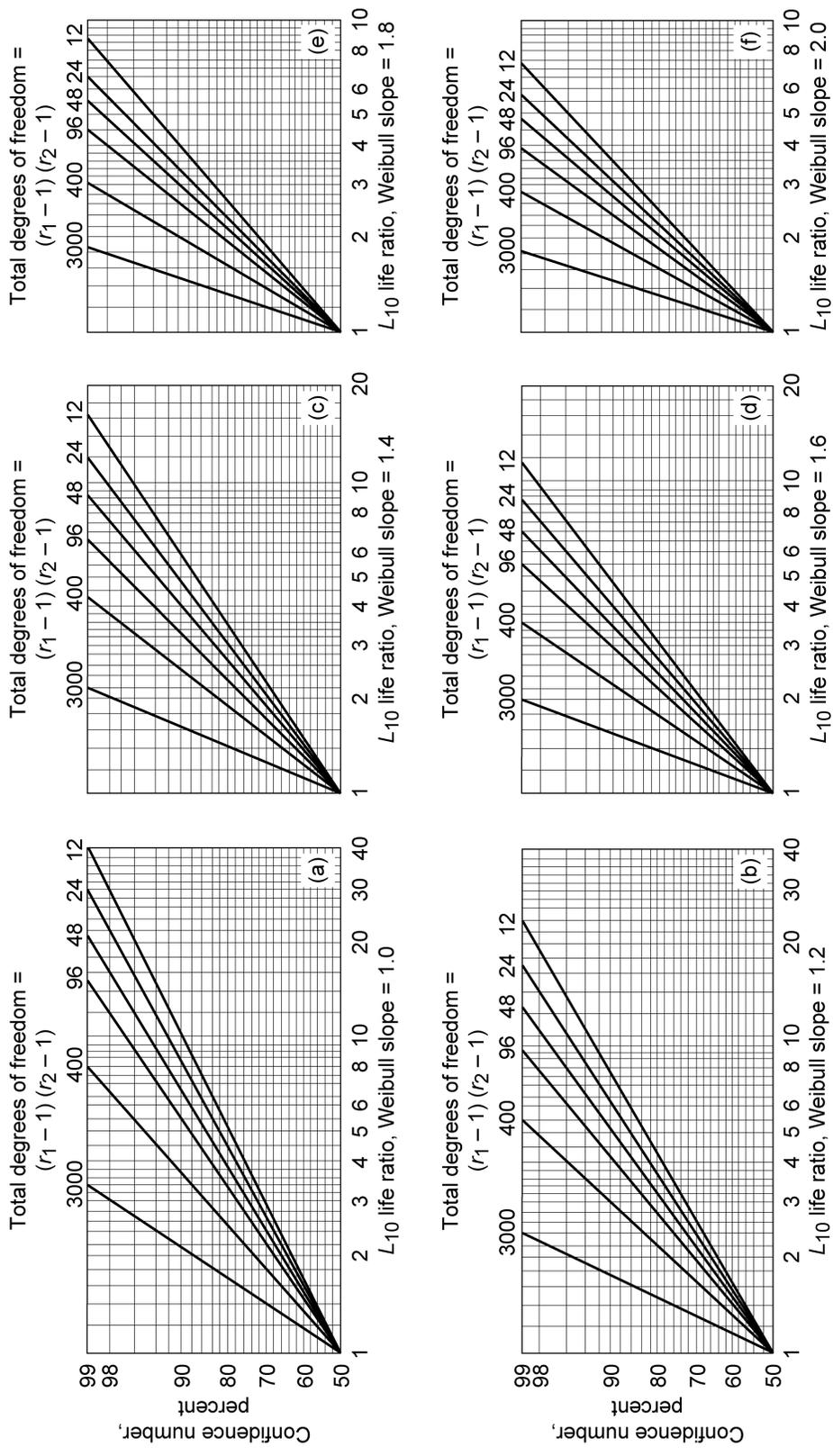
Figure 15.—Confidence numbers as a function of L_{10} life ratio and total degree of freedom (Ref. 10).

The quantity $(r_1 - 1)$ is known as the number of degrees of freedom for Lot 1. There are $(r_1 - 1)$ degrees of freedom because for a fixed value of failures r_1, only $(r_1 - 1)$ can be chosen arbitrarily, the last one being determined from the remaining values. Similarly, $(r_2 - 1)$ is the number of degrees of freedom in Lot 2. The product of $[(r_1 - 1)(r_2 - 1)]$ is the total degrees of freedom of the pair of lots.

Referring to the Weibull plots of Figure 14,

$$r_1 = \text{number of failures of Lot 1} = 7$$

$$r_2 = \text{number of failures of Lot 2} = 10$$

Thus, the total degrees of freedom $= (7 - 1)(10 - 1) = 54$.

The Weibull slopes of both lots are approximately 1.7 and the L_{10} life ratio equals 76/38 or 2. Interpolating between Figures 15(d) and (e) for 54 degrees of freedom at Weibull slopes of 1.6 and 1.8, the confidence numbers are 75 and 78 percent, respectively. At a Weibull slope of 1.7 the average confidence number is 76.5 percent $[(75 + 78)/2]$. This indicates that there are 765 chances out of 1000 that the L_{10} life in the population of Lot 2 is superior to the L_{10} life in the population of Lot 1. (A 95-percent confidence number is equivalent to 2σ confidence band while a 68-percent confidence number is equivalent to a 1σ confidence band.) In general, it is desirable to have a confidence number of 90 or greater to assure a statistically significant difference between two populations.

If Lots 1 and 2 have unequal Weibull slopes, the confidence number can be determined by treating the two lots as if both had the Weibull slope of Lot 1. Then obtain a second confidence number by treating both lots as if both had a Weibull slope of Lot 2. To arrive at the true confidence number the two results are averaged together (Ref. 10).

To determine the confidence number for successive comparisons or successive tests, Johnson (Ref. 10) provides the following formula

$$C = 1 - 2^{n-1} \prod_{i=1}^{n} (1 - C_i) \tag{11}$$

As an example, suppose there is a second set of tests to compare Lots 1 and 2, for the second set of tests, the resultant confidence number is 0.8. Then from Equation (11), the combined confidence number is

$$C = 1 - 2(1-C_1)(1-C_2) = 1 - 2(1 - 0.765)(1 - 0.8) = 0.906 \tag{12}$$

Assume that there is a third set of data that provides a confidence number of 0.65. The combined confidence number is

$$\begin{aligned} C = 1 - 2^{(3-1)}(1-C_1)(1-C_2)(1-C_3) = \\ 1 - 4(1 - 0.765)(1 - 0.8)(1 - 0.65) = 0.934 \end{aligned} \tag{13}$$

From the above, it may be concluded with reasonable engineering and statistical certainty that Lot 2 will provide a longer rolling-element fatigue life than Lot 1 approximately 93 percent of the time. However, there will be instances (approximately 7 percent of the time) where the population of Lot 1 will give longer lives.

Determining Significance of Test Results

If the data being compared is from either full-scale bearing tests or bench-type tests, confidence numbers can be used. The previously established rules based on variation in life, however, should only be applied to full-scale bearing testing where the lives of a bearing population with which the experimental or field data are to be compared are known and/or predicted. However, there are instances where there are test results where there are either insufficient test failures and/or the ratio of the life results are not sufficient to conclude with any reasonable engineering and/or statistical certainty that life differences in the variables being tested exist. This can occur where a single variable is being tested such as material chemistry, additive and lubricant chemistry, material hardness, etc.

For purposes of example, let us assume that there appears to be a relation between the volume of an additive present in a lubricant and bearing fatigue life. In this example we will assume that in four test series life increases with increases in additive content where Test Series D with the highest percentage of additive gives the longest life and Test Series A with no additive present gives the lowest life. Test Series C has an additive content greater than Test Series B but less than Test Series D. The order of the test results from longest life to shortest life are D, C, B, and A. However, the confidence number between Test Series D and A is less than 90 percent. It may be possible to combine the confidence numbers as discussed in the previous section to obtain a confidence number greater than 90 percent showing an effect of additive volume on fatigue life. Alternatively, the following formula may be used.

$$\text{Percent Probability of a Relation Existing} = [1-1/(n!)] \times 100 \qquad (14)$$

where n is the number of test series or groups.

In the example above, $n = 4$ and factorial $(n!) = 4 \times 3 \times 2 \times 1 = 24$. From Equation (14) there is a 96 percent probability that there exists a relation between additive volume percent and fatigue life. However, assume that there were only three test series whereby $(n!) = 3 \times 2 \times 1 = 6$. From Equation (14) there is an 83 percent probability that there exists a relation between additive volume percent and fatigue life. This percentage may be insufficient to conclude with any statistical certainty that a relation does exist.

Summary

In order to rank bearing materials, lubricants and design variables using rolling-element bench type fatigue testing and rolling-element bearing tests, the investigator needs to be cognizant of the variables that affect rolling-element fatigue life and be able to maintain and control them within an acceptable experimental tolerance. This paper brings together and discusses the technical aspects of rolling-element fatigue testing and data analysis as well as making recommendations to assure quality and reliable testing of rolling-element specimens and full-scale rolling-element bearings. These are as follows:

1. When testing to obtain valid comparison of the lubricant, material, and/or operating variables in bench-type rolling-element fatigue testers, all the rolling-element specimens must fabricated from a single heat of material, heat treated simultaneously to the same hardness. All specimens must have the same surface finish unless the surface finish is the parameter being studied. The steel microstructure should be reported together with the retained austenite and residual stress before and after testing. It is of prime importance that the difference in hardness between the contacting test specimens remains constant.
2. Where high reliability is desired for a given application it is preferable to test a group of bearings to determine their actual lives. In such cases, the same precautions should be taken as with a bench-type tester discussed above. In general, test stresses lower than 2.4 GPa (350 ksi)

maximum Hertz are suggested. However, maximum Hertz stresses as high as 3.1 GPa (450 ksi) on the inner race can be used for testing many types of bearings.

3. The interference fit between the bearing bore and the shaft needs to be controlled and reported. The interference fit can change the bearing's internal diametrical clearance and will also induce tensile hoop stresses in the bearing inner race. These tensile stresses can increase the magnitude of shearing stresses below the contacting surface between the rolling elements and the bearing inner race and reduce the bearing fatigue life. It can also alter the Hertz stress-life relation.

4. Comparisons show that bench-type fatigue testers can reliably identify qualitative effects of many variables on rolling-element fatigue life. By bench marking these life results to an already existing data base, it is possible to develop bearing life modifying factors with the Lundberg-Palmgren theory to predict bearing life with reasonable engineering certainty.

5. Reductions up to 40 percent in bearing test time and calendar time can be achieved by testing half of the specimens to failure or to the L_{50} life and terminating all testing when the last of the predetermined bearing failures have occurred. Sudden death testing is not a more efficient method to reduce bearing test time or calendar time when compared to censored sequential testing.

6. Once variables are controlled, the number of tests and the test conditions need to be specified to assure reasonable statistical certainty of the final results. Using the statistical methods of W. Weibull and L. Johnson, the minimum number of tests required can be determined.

Appendix A.—Effect of Gross Plastic Deformation on Contact Radii

For many applications where gross plastic deformation occurs, it is necessary to calculate the effective Hertz stress or the stress after plastic deformation (Ref. 17). This can be accomplished by deriving the radius of curvature R_p of the deformed rolling element as follows:

Referring to Figure 5(a) let

$$A = \frac{1}{2} H(2l) \tag{A1}$$

approximately, then

$$h' = h + H \ \ \text{or} \ \ h = h' - H \tag{A2}$$

Then

$$\begin{aligned} l^2 &= R_p^2 - (R - h)^2 \\ &= 2R_p h - h^2 \end{aligned} \tag{A3}$$

and

$$R_p = \frac{l^2 + h^2}{2h} \tag{A4}$$

If $R_p = R$ and $h = h'$, Equation (A3) becomes

$$\left. \begin{aligned} l &= 2Rh' - (h')^2 \\ &\text{and} \\ h' &= R \pm \left(R^2 - x^2\right)^{1/2} \end{aligned} \right\} \tag{A5}$$

Substituting Equation (A5) into Equation (A2) and solving for h in terms of A, R, and H results in

$$h = R \pm \left[R^2 - \left(\frac{A}{H}\right)^2 \right]^{1/2} - H \tag{A6}$$

If H is substituted into Equation (A4) and a negative sign selected for the radical in Equation (A6),

$$R_p = \frac{\left(\dfrac{A}{H}\right)^2 + \left\{ R - \left[R^2 - \left(\dfrac{A}{H}\right)^2 \right]^{1/2} - H \right\}^2}{2\left\{ R - \left[R^2 - \left(\dfrac{A}{H}\right)^2 \right]^{1/2} - H \right\}} \tag{A7}$$

Since $\left\{R - \left[R^2 - \left(\dfrac{A}{H}\right)^2\right]^{1/2} - H\right\}^2$ is small relative to $\left(\dfrac{A}{H}\right)^2$, it can be neglected in the numerator, then

$$R_p = \frac{\left(\dfrac{A}{H}\right)^2}{2\left\{R - \left[R^2 - \left(\dfrac{A}{H}\right)^2\right]^{1/2} - H\right\}} \tag{A8}$$

The deformed radius R'_p (not shown) in the plane perpendicular to the plane of the profile shown in Figure 5(a) is

$$R'_p = R' - H$$

where R' is the radius of the body in the perpendicular plane. Since H is extremely small relative to R',

$$R'_p = R' \tag{A10}$$

Substituting R_p in the Hertzian equations will give the effective compressive Hertz stress after gross plastic deformation of the rolling-element surface.

For a race groove surface having a concave or negative radius R, as shown in Figure 5(b),

$$R_p = \frac{\left(\dfrac{A}{H}\right)^2}{2\left\{R - \left[R^2 - \left(\dfrac{A}{H}\right)^2\right]^{1/2} + H\right\}} \tag{A11}$$

The area of deformation A and track depth H can be measured directly from a surface contour trace.

Appendix B.—Sudden Death Testing Techniques

As discussed by Vlcek, Hendricks, and Zaretsky (Ref. 33), in sudden death testing, the total number of specimens to be evaluated is divided into equal subgroups that can be evaluated simultaneously. The first subgroup of specimens is run simultaneously until the first failure occurs. The surviving tests are terminated (i.e., suspended), and new test specimens are mounted in the testers. This process is repeated until all of the test specimens in the population have been screened. A technique developed by Vlcek, Zaretsky, and Hendricks (Ref. 32) was used to generate virtual bearing sets that were analyzed as if they were sudden death tested. Total populations with 36, 72, and 144 deep-groove bearings were generated. The populations were then sequentially broken into subgroups representing all possible combinations of sudden death test series of ($m \times r$), where m was the number of bearing testers used simultaneously and r was the number of sets of m bearings necessary to achieve the total number of bearings n in the total population. The total number of bearings n equal m times r. For example, if 36 bearings were to be evaluated, and there were 4 bearing fatigue testers available, the value of m would be 4 while the value of r would be 9; whereby n equals 36 (4×9). For this example, the first four bearings were run simultaneously until the first failure occurred. The three surviving tests were suspended, and four new bearings were mounted. This process was repeated until nine failures occurred; one from each of the sets of 4, with ($m - 1) \times r$ or 27 suspensions.

These nine failures and their corresponding median ranks, one for each subgroup of size m, were then plotted on a Weibull plot. This is illustrated as Step 1 in the schematic of a generic Weibull plot of the sudden death line (SDL) of Figure 16. This SDL represents the distribution of first failures in each subgroup. The SDL of each series was next shifted on its respective Weibull plot, Steps 2 and 3 of Figure 16, so that the curve represented the failures of the total population, not just that of one out of r bearings.

Various methods exist for shifting the SDL (Fig. 16) and finding the life of a total population n based upon sudden death testing data where only r failures are considered. The slope and characteristic life of the subpopulation generated during sudden death testing can be found from maximum likelihood estimators of Cohen (Ref. 35) that are obtained from an iterative process. This life for r samples must be corrected to represent the life of the original population containing n samples. One way to achieve this, as reported by McCool (Ref. 36) is to multiply the subpopulation life estimator by the number of samples (m) in each equally sized subpopulation raised to the inverse of the slope estimator. Confidence limits can be placed upon these values for a limited number of cases provided in tables in the open literature or by
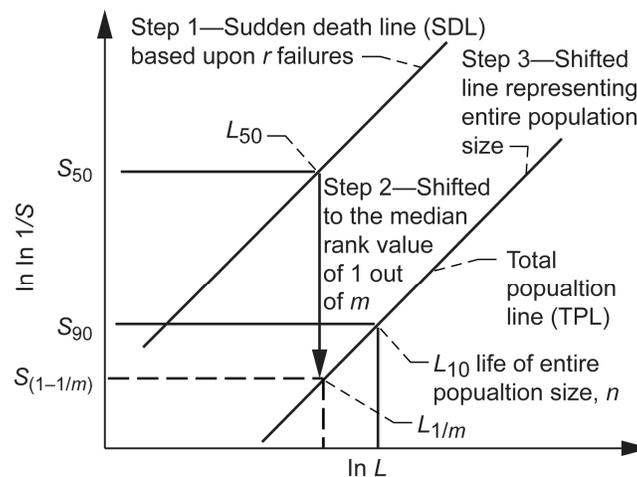

Figure 16.—Schematic of generic Weibull plot of the sudden death line shifted to total population line (Ref. 33).

extensive Monte Carlo simulations (Ref. 36). Houpert (Ref. 37) also proposes a technique for determining the life of a larger population based upon a sub-population determined from sudden death testing.

For its simplicity of application and relative engineering accuracy, we prefer a technique presented in Johnson (Ref. 10) for shifting the SDL so that the life and characteristics of the larger bearing population (n) can be projected. The generic Weibull plot of Figure 16 accompanies the following steps, and includes many of the elements mentioned.

(Step 1) *Plotting the subgroup of r failures on Weibull paper.* To plot the failures, median ranks are assigned to the sequentially ordered lives. Median ranks were defined using

$$\text{median rank} = (j - 0.3)/(r + 0.4) \tag{B1}$$

where $j = 1, 2, 3, \ldots r$. For sudden death testing, the number of subsets r equal n. A discussion and comparison of median rank definitions is available in Houpert (Ref. 37) and Skinner et al. (Ref. 37). The median ranks along with their corresponding lives are next plotted on Weibull paper. The locus of points is fitted with a linear curve. From the Weibull plot the Weibull slope, the L_{10} life, L_{50} life and characteristic life, L_β, are determined. This SDL represents the distribution of first failures at the median rank for one failure out of the number of samples (m) in each of the subgroups.

(Step 2) Determining by how much the SDL must be shifted to accurately estimate the L_{10} life for the entire population. The median rank (Eq. (B1)) must be determined for the first failure out of the number of bearings simultaneously evaluated (m). In the above example, for a $[(m = 4) \times (r = 9)]$ test, the four simultaneous testers are stopped after the first test failure occurs, thus the mean order number $j = 1$ and the subgroup size $m = 4$ where it is assumed that in Equation (B1) $m = r$. The median rank for 1 out of 4, found using Equation (B2) below is 0.1591. This is the value to which the SDL must be shifted (Fig. 16). In general,

$$\text{First failure median rank (FFMR)} = (1 - 0.3)/(m + 0.4) \tag{B2}$$

(Step 3) *Constructing the Total Population Line (TPL) by shifting the SDL.* At the L_{50} intersection of the SDL, a vertical line is drawn down to the median rank value determined in Step 2. Through this point, a line is drawn parallel to the SDL created in Step 1. The slopes of both lines are assumed to be equal. Figure16 is a generic Weibull plot of the SDL and the shifted Total Population Line (TPL) representative of this technique.

(Step 4) *Determining lives from the shifted TPL.* The Weibull slope and lives are read directly from the TPL generated in Step 3. Table 3 contains the Weibull slope, L_{10} life, L_{50} life, and Characteristic life, L_β, for a typical $[(m = 4) \times (r = 9)]$ sudden death test of a virtual deep groove bearing. The values obtained from the SDL and the shifted TPL are provided.

TABLE 3.—COMPARISON BETWEEN LIVES OBTAINED FROM
MONTE CARLO SUDDEN DEATH TESTING AND THAT
ADJUSTED FOR TOTAL POPULATION
[Number of failures, 9; number of bearings tested, 36; number
of test rigs, 4; assumed Weibull slope, 1.11; resultant Weibull
slope, 1.033; bearing size and type, 50-mm bore deep-groove
ball bearing (Ref. 33).]

Bearing population size	Bearing life, hr			Weibull slope, e
	L_{10}	L_{50}	L_β	
Sudden death for 9 failures	2354	14569	20772	1.033
Adjusted for total population from sudden death	9003	55729	79453	1.033
Calculated[a] (actual) for total population	6912	37729	47729	1.11

[a]Life based on Zaretsky's rule and lubricant life factor (Ref. 1).

Appendix C.—Derivation of Strict Series Reliability

As discussed and presented in References 39 and 40, G. Lundberg and A. Palmgren (Ref. 31) in 1947, using the Weibull Equations (Refs. 8 and 9) for rolling-element bearing life analysis, first derived the relationship between individual bearing component lives and bearing system L_{10} life. The following derivation is based on but is not identical to the Lundberg-Palmgren analysis (Ref. 31) which did not include the rolling-element (ball or roller) set life.

Referring to Figure 10(a) and Equation (6), the Weibull equation can be written as

$$\ln\ln\left[\frac{1}{S_{\mathrm{x}}}\right] = e\ln\left[\frac{L}{L_{\beta}}\right] \tag{C1}$$

where L is the number of cycles to failure at a probability of survival of S_{x}. The characteristic life L_{β} is the life at a 36.8 percent probability of survival or a 63.2 $[(1 - 0.368) \times 100 = 63.2]$ percent probability of failure.

Figure 17 is a sketch of multiple Weibull plots where each Weibull plot represents a cumulative distribution of the bearing and each component of the bearing system. The Weibull plot of the bearing represents the combined Weibull plots of the (1) inner race, (2) rolling-element set, and (3) outer race. All plots are assumed to have the same Weibull slope e. The slope e can be defined as follows:

$$e = \frac{\ln\ln\left[\frac{1}{S_{\mathrm{x}}}\right] - \ln\ln\left[\frac{1}{S_{90}}\right]}{\ln L - \ln L_{10}} \tag{C2a}$$

or

$$\frac{\ln\left[\frac{1}{S_{\mathrm{x}}}\right]}{\ln\left[\frac{1}{S_{90}}\right]} = \left[\frac{L}{L_{10}}\right]^{e} \tag{C2b}$$

From Equations (C1) and (C2b),

$$\ln\left[\frac{1}{S_{\mathrm{x}}}\right] = \left[\ln\frac{1}{S_{90}}\right]\left[\frac{L}{L_{10}}\right]^{e} = \left[\frac{L}{L_{\beta}}\right]^{e} \tag{C3}$$

and

$$S_{\mathrm{x}} = \exp-\left[\frac{L}{L_{\beta}}\right]^{e} \tag{C4}$$

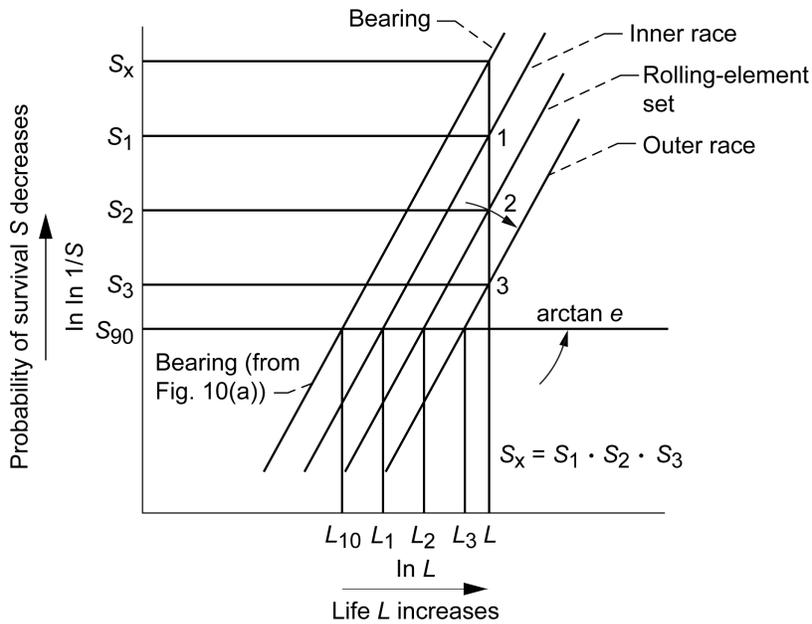where Equation (C4) is identical to Equation (C1).

Figure 17.—Sketch of multiple Weibull plots where each numbered plot represents cumulative distribution of each component of the bearing. Weibull plot designated as "Bearing" represents combined distribution of plots 1, 2, and 3 (all plots are assumed to have same Weibull slope e) (Ref. 39).

For a given time or life L, each component in a system will have a different reliability S. For a series reliability system the probability of survival of the system S_x at a given time or life L is the product of the probabilities of survival of each of the components making up the system where for a bearing

$$S_x = S_1 \cdot S_2 \cdot S_3 \tag{C5}$$

Combining Equations (C4) and (C5) gives

$$\exp - \left[\frac{L}{L_\beta}\right]^e = \exp - \left[\frac{L}{L_{\beta 1}}\right]^e \times \exp - \left[\frac{L}{L_{\beta 2}}\right]^e \times \exp - \left[\frac{L}{L_{\beta 3}}\right]^e \tag{C6a}$$

$$\exp - \left[\frac{L}{L_\beta}\right]^e = \exp - \left\{ \left[\frac{L}{L_{\beta 1}}\right]^e + \left[\frac{L}{L_{\beta 2}}\right]^e + \left[\frac{L}{L_{\beta 3}}\right]^e \right\} \tag{C6b}$$

It is assumed that the Weibull slope e is the same for all components. From Equation (C6b)

$$-\left[\frac{L}{L_\beta}\right]^e = -\left\{ \left[\frac{L}{L_{\beta 1}}\right]^e + \left[\frac{L}{L_{\beta 2}}\right]^e + \left[\frac{L}{L_{\beta 3}}\right]^e \right\} \tag{C7a}$$

Factoring out L from Equation (C7a) gives

$$\left[\frac{1}{L_\beta}\right]^e = \left[\frac{1}{L_{\beta1}}\right]^e + \left[\frac{1}{L_{\beta2}}\right]^e + \left[\frac{1}{L_{\beta3}}\right]^e \tag{C7b}$$

From Equation (C3) the characteristic lives $L_{\beta1}$, $L_{\beta2}$, $L_{\beta3}$, etc., can be replaced with the respective lives L_1, L_2, and L_3, at S_{90} (or the lives of each component that have the same probability of survival S_{90}) as follows:

$$\left[\ln\frac{1}{S_{90}}\right]\left[\frac{1}{L_{10}}\right]^e = \left[\ln\frac{1}{S_{90}}\right]\left[\frac{1}{L_1}\right]^e + \left[\ln\frac{1}{S_{90}}\right]\left[\frac{1}{L_2}\right]^e + \left[\ln\frac{1}{S_{90}}\right]\left[\frac{1}{L_3}\right]^e \tag{C8}$$

where, in general, from Equation (C3)

$$\left[\frac{1}{L_\beta}\right]^e = \left[\ln\frac{1}{S_{90}}\right]\left[\frac{1}{L_{10}}\right]^e \tag{C9a}$$

and

$$\left[\frac{1}{L_{\beta1}}\right]^e = \left[\ln\frac{1}{S_{90}}\right]\left[\frac{1}{L_1}\right]^e, \text{etc.} \tag{C9b}$$

Factoring out $\left[\ln\dfrac{1}{S_{90}}\right]$ from Equation (C8) gives

$$\left[\frac{1}{L_{10}}\right] = \left\{\left[\frac{1}{L_1}\right]^e + \left[\frac{1}{L_2}\right]^e + \left[\frac{1}{L_3}\right]^e\right\}^{1/e} \tag{C10}$$

or rewriting Equation (C10) results in

$$\left(\frac{1}{L_{10}}\right)^e = \left(\frac{1}{L_{\text{ir}}}\right)^e + \left(\frac{1}{L_{\text{re}}}\right)^e + \left(\frac{1}{L_{\text{or}}}\right)^e \tag{C11}$$

Equation (C11) is identical to Equation (7b) of the text.

References

1. Zaretsky, E.V., Ed., (1992), STLE Life Factors for Rolling Bearings, STLE SP–34, Society of Tribologists and Lubrication Engineers, Park Ridge, IL.
2. Sadeghi, F.; Jalalahmadi, B., Slack, T.S., Raje, N., and Arakere, N.K., (2009), "A Review of Rolling Contact Fatigue," Jour. of Tribology, ASME Trans., 131, 4, Art. No. 041403, OCT 2009.
3. Alley, E.S., and Neu, R.W., (2010) "Microstructure-Sensitive Modeling of Rolling Contact Fatigue," International Jour. of Fatigue, 32, 5: pp. 841–850.
4. Zaretsky, E.V., Ed., (1997), Tribology for Aerospace Applications, STLE SP–37, Society of Tribologists and Lubrication Engineers, Park Ridge, IL.
5. Stribeck, R., (1900), "Reports From the Central Laboratory for Scientific Investigation," Translation by H. Hess, 1907, ASME Trans., 29, pp. 420–466.
6. Moult, J.F., (1963) "Critical Aspects in Bearing Fatigue Testing," J. ASLE (now STLE), (Dec. 1963), pp. 503–511.
7. Bamberger, E.N., Harris, T.A., Kacmarsky, W.M., Moyer, C.A., Parker, R.J., Sherlock, J.J., and Zaretsky, E.V., (1971), Life Adjustment Factors for Ball and Roller Bearings, An Engineering Design Guide, ASME, New York.
8. Weibull, W., (1939), "A Statistical Theory of the Strength of Materials," Inginiors Vetenskaps Adademien (Proc. Royal Swedish Academy of Engr.), 151.
9. Weibull, W., (1939), "The Phenomenon of Rupture," Inginiors Vetenskaps Adademien (Proc. Royal Swedish Academy of Engr.), 153.
10. Johnson, L.G., (1964), The Statistical Treatment of Fatigue Experiments, Elsevier Publishing Co., Amsterdam.
11. Zaretsky, E.V., Parker, R.J., and Anderson, W.J., (1982), "NASA Five-Ball Fatigue Tester – Over 20 Years of Research," Rolling Contact Fatigue Testing of Bearing Steels, J.J.C. Hoo, Ed., ASTM STP 771, American Society of Testing Materials, Philadelphia, PA., pp. 5–45.
12. Hoo, J.J.C., (1982), Rolling Contact Fatigue Testing of Bearing Steels, ASTM STP 771, Philadelphia, PA.
13. McCool, J.I., and Valori, R., (2009), "Evaluating the Validity of Rolling Contact Fatigue Results," Tribology Transactions, 52, 2, pp. 223–230.
14. Zaretsky, E.V., Sibley, L.B., and Anderson, W.J., (1963), "The Role of Elastohydrodynamic Lubrication in Rolling-Contact Fatigue," Journal of Basic Engineering, Trans. ASME, Ser. D, 85, pp. 439–450.
15. Drutowski, R.C., and Mikus, E.B., (1960), "The Effect of Ball Bearing Steel Structure on Rolling Friction and Plastic Deformation," Journal of Basic Engineering, Trans. ASME, Ser. D, 82, pp. 302–308.
16. Drutowski, R.C., (1962), "The Linear Dependence of Rolling Friction on Stressed Volume," Rolling Contact Phenomena, J.B. Bidwell, ed., Elsevier, Amsterdam, pp. 113–131.
17. Zaretsky, E.V., Anderson, W.J., and Parker, R.J., (1962), "The Effect of Nine Lubricants on Rolling-Contact Fatigue Life," NASA TN D-1404.
18. Zaretsky, E.V., Anderson, W.J., and Parker, R.J., (1962), "The Effect of Contact Angle on Rolling-Contact Fatigue and Bearing Load Capacity," ASLE Transactions, 5, pp. 210–219.
19. International Organization for Standardization (ISO), (2006), "Rolling Bearings-Static Load Ratings," ISO 76:2006, International Organization for Standardization, Geneva, Switzerland.
20. Chen, W.W., Wang, Q.J., Wang, F., Keer, L.M., and Cao, J., (2008), "Three-dimensional Repeated Elasto-Plastic Point Contacts, Rolling, and Sliding," J. Appl. Mech., Trans. ASME, 75, 2: Art. No. 021021 MAR 2008.
21. Nelias, D., Antaluca, E., Boucly, V., Cretu, S., (2007), "A three-dimensional semianalytical model for elastic-plastic sliding-contacts," J. Tribology, Trans. ASME, 129, 4, pp. 761–771.
22. Nelias, D., Antaluca, E., Boucly, V., (2007), "Rolling of an elastic ellipsoid upon an elastic-plastic flat," J. Tribology, Trans. ASME, 129, 4, pp. 791–800.

23. Wang, F.S., Block, J.M., Chen, W.W., Martini, A., Zhou, K., Keer, L.M., Wang, Q.J., (2009), "A Multilevel Model for Elastic-Plastic Contact Between a Sphere and a Flat Rough Surface," J. Tribology, Trans. ASME, 131, 2: Art. No. 021409 APR 2009.

24. Galbato, A.T., (1982), "Methods of Testing for Rolling Contact Fatigue of Bearing Steels," Rolling Contact Fatigue Testing of Bearing Steels, J.J.C. Hoo, Ed., ASTM STP 771, American Society of Testing Materials, Philadelphia, PA., pp. 169–189.

25. Coe, H.H., and Zaretsky, E.V., (1986), Effect of Interference Fits on Roller Bearing Fatigue Life," ASLE Transactions, 30, 2, pp. 131–140.

26. Oswald, F.W., and Zaretsky, E.V., and Poplawski, J.V., (2009), "Interference Fit Life Factors for Roller Bearings," Tribology Trans., 52, 3, pp. 415–426.

27. Oswald, F.W., and Zaretsky, E.V. and Poplawski, J.V., (2011), "Interference Fit Life Factors for Ball Bearings," Tribology Trans., 54, 1, pp. 1–20.

28. Zaretsky, E.V., Parker, R.J. and Anderson, W.J., (1967), "Component Hardness Differences and Their Effect on Rolling-Element Fatigue Life," ASME Trans., Jour. Lubrication Technology, 89, 1, pp. 47–62.

29. Parker, R.J. and Zaretsky, E.V., (1972), "Rolling-Element Fatigue Lives of Through Hardened Bearing Materials," ASME Trans., Jour. Lubrication Technology, 94, 2, pp. 165–173.

30. Bamberger, E.N., and Zaretsky, E.V., (1971), "Fatigue Lives at 600 °F of 120- Millimeter-Bore Ball Bearings of AISI M-50, AISI M-1 and WB-49 Steels," NASA TN D-6156, National Aeronautics and Space Administration, Washington, DC.

31. Lundberg, G., and Palmgren, A., (1947,) "Dynamic Capacity of Rolling Bearings," Acta Polytechnica Mechanical Engineering Series, 1, 3, Stockholm, Sweden.

32. Vlcek, B.L., Hendricks, R.C., and Zaretsky, E.V., 2003, "Determination of Rolling-Element Fatigue Life from Computer Generated Bearing Tests," STLE Tribology Trans., 46, 3, pp. 479–493.

33. Vlcek, B.L., Hendricks, R.C., and Zaretsky, E.V., (2004), "Monte Carlo Simulation of Sudden Death Bearing Testing," Tribology Trans., 47, 2, pp. 188–199.

34. Lieblein, J., (1954), "A New Method of Analyzing Extreme-Value Data," NACA TN 3053.

35. Cohen, C., (1965), "Maximum Likelihood Estimation in the Weibull Distribution Based on Complete and on Censored Samples," Technomet, 7, 4, pp. 579–588.

36. McCool, J., (1982), "Analysis of Sets of Two-Parameter Weibull Data Arising in Rolling Contact Endurance Testing," Rolling Contact Fatigue Testing of Bearing Steels, J.J.C. Hoo, Ed., ASTM STP 771, American Society of Testing Materials, Philadelphia, PA., pp. 293–319.

37. Houpert, L., (2003), "An Engineering Approach to Confidence Intervals and Endurance Test Strategies," STLE Tribology Trans., 46, 2, pp. 248–259.

38. Skinner, K., Keates, J. and Zimmer, W., (2001), "A Comparison of Three Estimators of the Weibull Parameters," Quality and Reliability Engineering International, 17, pp. 249–256.

39. Poplawski, J.V., Peters, S.M., and Zaretsky, E.V., (2001), "Effect of Roller Profile on Cylindrical Roller Bearing Life Prediction—Part I: Comparison of Bearing Life Theories," STLE Tribology Trans., 44, 3, pp. 339–350.

40. Poplawski, J.V., Peters, S.M., and Zaretsky, E.V., (2001), "Effect of Roller Profile on Cylindrical Roller Bearing Life Prediction—Part II: Comparison of Roller Profiles," STLE Tribology Trans., 44, 3, pp. 417–427.

REPORT DOCUMENTATION PAGE					Form Approved OMB No. 0704-0188
The public reporting burden for this collection of information is estimated to average 1 hour per response, including the time for reviewing instructions, searching existing data sources, gathering and maintaining the data needed, and completing and reviewing the collection of information. Send comments regarding this burden estimate or any other aspect of this collection of information, including suggestions for reducing this burden, to Department of Defense, Washington Headquarters Services, Directorate for Information Operations and Reports (0704-0188), 1215 Jefferson Davis Highway, Suite 1204, Arlington, VA 22202-4302. Respondents should be aware that notwithstanding any other provision of law, no person shall be subject to any penalty for failing to comply with a collection of information if it does not display a currently valid OMB control number. PLEASE DO NOT RETURN YOUR FORM TO THE ABOVE ADDRESS.					
1. REPORT DATE (DD-MM-YYYY) 01-03-2011		2. REPORT TYPE Technical Memorandum		3. DATES COVERED (From - To)	
4. TITLE AND SUBTITLE Rolling-Element Fatigue Testing and Data Analysis--A Tutorial				5a. CONTRACT NUMBER	
				5b. GRANT NUMBER	
				5c. PROGRAM ELEMENT NUMBER	
6. AUTHOR(S) Vlcek, Brian, L.; Zaretsky, Erwin, V.				5d. PROJECT NUMBER	
				5e. TASK NUMBER	
				5f. WORK UNIT NUMBER WBS 432938.11.01.03.02.02.16	
7. PERFORMING ORGANIZATION NAME(S) AND ADDRESS(ES) National Aeronautics and Space Administration John H. Glenn Research Center at Lewis Field Cleveland, Ohio 44135-3191				8. PERFORMING ORGANIZATION REPORT NUMBER E-16955-1	
9. SPONSORING/MONITORING AGENCY NAME(S) AND ADDRESS(ES) National Aeronautics and Space Administration Washington, DC 20546-0001				10. SPONSORING/MONITOR'S ACRONYM(S) NASA	
				11. SPONSORING/MONITORING REPORT NUMBER NASA/TM-2011-216098	
12. DISTRIBUTION/AVAILABILITY STATEMENT Unclassified-Unlimited Subject Category: 37 Available electronically at http://www.sti.nasa.gov This publication is available from the NASA Center for AeroSpace Information, 443-757-5802					
13. SUPPLEMENTARY NOTES					
14. ABSTRACT In order to rank bearing materials, lubricants and other design variables using rolling-element bench type fatigue testing of bearing components and full-scale rolling-element bearing tests, the investigator needs to be cognizant of the variables that affect rolling-element fatigue life and be able to maintain and control them within an acceptable experimental tolerance. Once these variables are controlled, the number of tests and the test conditions must be specified to assure reasonable statistical certainty of the final results. There is a reasonable correlation between the results from elemental test rigs with those results obtained with full-scale bearings. Using the statistical methods of W. Weibull and L. Johnson, the minimum number of tests required can be determined. This paper brings together and discusses the technical aspects of rolling-element fatigue testing and data analysis as well as making recommendations to assure quality and reliable testing of rolling-element specimens and full-scale rolling-element bearings.					
15. SUBJECT TERMS Bearings; Roller bearings; Ball bearings; Rolling-element fatigue life					
16. SECURITY CLASSIFICATION OF:			17. LIMITATION OF ABSTRACT	18. NUMBER OF PAGES	19a. NAME OF RESPONSIBLE PERSON STI Help Desk (email:help@sti.nasa.gov)
a. REPORT U	b. ABSTRACT U	c. THIS PAGE U	UU	41	19b. TELEPHONE NUMBER (include area code) 443-757-5802